An-Najah National University

Faculty of Graduate Studies

POLYURETHANE BASED FOAM FROM OLIVE MILL WASTEWATER: SYNTHESIS AND APPLICATION IN WASTEWATER PURIFICATION

By

Isra Ishraydeh

Supervisors

Prof. Othman Hamed

Dr. Abdel Fattah R. Hasan

This Thesis is Submitted in Partial Fulfillment of the Requirements for the Degree of Master of Environmental Sciences, Faculty of Graduate Studies, An-Najah National University, Nablus - Palestine.

2023

POLYURETHANE BASED FOAM FROM OLIVE MILL WASTEWATER: SYNTHESIS AND APPLICATION IN WASTEWATER PURIFICATION

By

Isra Ishraydeh

This Thesis was Defended Successfully on 21/2/2023 and approved by

Prof. Othman Hamed Supervisor	Othman Hamed Signature
Dr. Abdel Fattah R. Hasan Co-Supervisor	Signature
Dr. Anan Barghouthi External Examiner	Signature
Prof. Shehdeh Jodeh Internal Examiner	Shehdeh Jodeh Signature

Dedication

To the people who always have inspired me, I dedicate this work starting with my father who always urged me for more best work, and to my mother whose prayers were with me all the path to success. To my sisters and brothers, who encouraged me and were always a source of motivation. To my all friends for being there for me through my study in master's program specially Layali.

Acknowledgements

I'd like to begin my acknowledgment with my gratefulness to Allah for guiding me through this significant stage of life and always making it possible through all obstacles i faced. This study is the result of help and support from great people who stood with me when i needed them. All parts of this study have its fingerprint after a special teacher encourage me to achieve it. Starting with my supervisor Prof. Othman Hamed whom without none of this would achieve. I truly appreciate your help and guidance, not only demonstrated how to overcome difficulties, but he also developed thoughts and idea generators to get this work done.

I also want to address a deep thankful to Dr. Abdel Fattah R. Hasan for his service and outstanding teacher.

Additionally, I would like to express my gratitude to the Department of Chemistry at An-Najah National University and the Institute for Water and Environmental Studies, as well as their department heads, professors, and lab technicians, for their excellent support and resources provided to me throughout the course of my research, from the early stages to the testing and subsequent evaluation.

I want to thank everyone who helped make this study a success, both individuals and organizations. I might have forgotten certain names, but please know that I am deeply appreciated every effort that was done.

Declaration

I, the undersigned, declare that I submitted the thesis entitled:

POLYURETHANE BASED FOAM FROM OLIVE MILL WASTEWATER: SYNTHESIS AND APPLICATION IN WASTEWATER PURIFICATION

I declare that the work provided in this thesis, unless otherwise referenced, is the researcher's own work, and has not been submitted elsewhere for any other degree or qualification.

Student's Name: **Isra Ishraydeh**

Signature: 

Date: **21/2/2023**

List of Contents

List of Tables

List of Figures

List of Appendices

POLYURETHANE BASED FOAM FROM OLIVE MILL WASTEWATER: SYNTHESIS AND APPLICATION IN WASTEWATER PURIFICATION

By
Isra Ishraydeh
Supervisors
Prof. Othman Hamed
Dr. Abdel Fattah R. Hasan

Abstract

One of the most important challenges in the world is water contamination especially from heavy metal ions. The high effectiveness removal of heavy metal ions, even at trace levels, has proved particularly demanding for absorption procedures, which are also less expensive than traditional approaches. Absorbents that have undergone chemical modification often have increased surface area and a higher absorption capacity than unmodified absorbents.

The goal of this study is to identify a natural source and a simple low-cost method to make a new absorbent for the removal of toxic metal ions. Pb(II) ions from wastewater have been tested using a modified version of lignin obtained from natural waste. What makes this study new and commercially important is the use of waste material for making new adsorbent material.

This study examines the enzymatic degradation approaches of lignin present in olive industry liquid waste (OILW) and converted it to a polyurethane foam material with urethane functionality. Then, the foam material as an adsorbent for toxic metals from wastewater.

The prepared foams were characterized by using FT-IR and TGA to examine the type of functional groups present in the foam and to determine its thermal stability. The prepared lignin-based foam was evaluated as an adsorbent for Pb (II) present in water. Lead (II) was selected because it is one of the most toxic metal ions. The effect of various parameters such as Pb ion concentration, temperature, pH, adsorbent dosage, and contact

time were all evaluated to determine the optimum adsorption conditions. The optimal value of the investigated parameters for LHMDIC was around 7.5 pH, 50 mg dosage, 50.00 ppm concentration, and 5.00 min of contact time, at 10°C. The ideal conditions for LPDIC were pH 8, 50 mg dosage, 50.00 ppm concentration, 5 min contact duration, at 10°C of Pb.

The maximum removal efficiency was determined to be 99.95% for LHMDIC and 98.75% for LPDIC. This application for Pb (II) ion removal efficiency for a genuine sewage sample showed outstanding removal. The Pb (II) ion appears to follow pseudo-second-order in the Pb (II) ion adsorption on LHMDIC and LPDIC polymers because (R^2 = 0.9999) and (R^2 = 1), respectively. Both forms follow the Langmuir model, since both showed R^2 values near 1. The values of G° for both foams are negative, indicating that the Pb (II) ion adsorption on LPDIC polymers is spontaneous.

Keywords: Adsorption, OILW, Lead, lignin, LIPDIC, LHMDIC, Urethane foam, sewage, polymer, water pollution.

Chapter One
Introduction

Water is the planet's most abundant resource. It is estimated to account for roughly 70% of the earth's mass. Domestic, commercial, and agricultural uses account for more than one-third of all freshwaters that is edible and renewable on earth. Given that most of these activities pollute

water with a combination of synthetic and naturally occurring chemicals, it should come as no Adjust surprise that chemical pollution of natural water has grown to be a major public concern in

almost all countries of the globe. As more individuals pass away from it every day, the death rate from drinking contaminated water has risen over time [1] [2].

1.1 Water Pollution

Both industrialized and developing countries are concerned about water contamination, specifically the influx of heavy metals into the aquatic environment. The environment and human health are both puts at risk due to the numerous factors that affect water quality, including human activity, vegetation, geology, soil type, climate, precipitation, flow conditions, and groundwater [3]. The main threat to the quality of the water comes from point sources from municipalities and industries. The quality of the water is impacted by mining, urbanization, and agriculture. Examples of non-point source contamination include hazardous contaminants, sediments, and nutrients [4].

Water pollution comes from a variety of sources, such as the battery and plating industries, heavy metal mining, fertilizers, pesticides, and paints, among others. Water contamination occurs when contaminants penetrate ecosystems and move up the food chain to humans. Heavy metal contamination is one of the most damaging contaminants due to its toxicity and bioaccumulation. Due to their persistence and lack of biodegradability, heavy metals pose serious problems when they accumulate in aquatic ecosystems [5].

Researchers have used a variety of approaches to purify contaminated water, one of the most significant environmental pollutants, due to the dangers of heavy metals and their harmful effects on both people and the environment.

However, due to adsorption techniques, easy operations, and low performance, several experiments and research have demonstrated that adsorption is one of the most successful ways to remove heavy metals from contaminated water [6-11].

1.2 Heavy Metals

Heavy metals are those with atomic weights ranging from 63.5 to 200.6 g/mol and density more than 5 g/cm³ [12]. While high quantities of heavy metals are regarded as dangerous, low concentrations are required for the metabolism of living things [13].

If a metal species was formed in an adverse environment, or if it was present in a form or concentration that had a detrimental effect on people or the ecosystem, it could be categorized as a "contaminant". All metals are exceedingly poisonous at large doses, and massive quantities can be harmful to the body. Plutonium, mercury, and lead are three additional harmful heavy metals that have no fundamentally beneficial or necessary effects on living things but whose accumulation in cells over time can cause major disorders [14].

The toxicity of heavy metals is influenced by a number of variables, including the duration of exposure, the characteristics of the metal species, and the physicochemical underpinnings [15].

1.2.1 Lead

Lead is a naturally occurring heavy, soft, and thin ash metal with a negligible amount in the crust [16, 17].

The World Health Organization (WHO) states that 0.01 mg/L is the maximum permissible value for lead (II) metal ions in water [18]. Batteries, pulp and paper, petrochemicals, oil refineries, printing, pigments, photographic materials, explosives production, ceramics, glass, paints, oil, metals, phosphorus fertilizers, electronics, wood production, and fossil fuel combustion, forest fires, mining operations, motor vehicle discharges, sewage, marine spraying, and many other things all use lead on a regular basis [19].

[17]. Lead absorption in human is influenced by a variety of variables, including age and physiological state. The kidneys absorb the largest amount of lead, followed by the liver, the heart, and the brain Numerous illnesses, including anemia, kidney problems, damage to the brain's cells, and even death with excessive poisoning are brought on by this metal [16].

1.3 Traditional Methods for Removing Heavy Metals

Water pollution from heavy metals threatens both the ecosystem's quality and human health. Reduced levels of heavy metals in surface waters and wastewater are necessary for

environmental preservation. Potential resources for removing heavy metals include, for example, fly ash, lignite, pine bark, and lignin, which are all types of industrial or agricultural waste [20].

The disadvantages of these methods include difficulties in conforming to strict regulatory standards with chemical precipitation and significant operational costs associated with activated carbon adsorption. In-depth research has therefore been done to develop metal adsorbents that are both more effective and less expensive. Many conventional techniques, including chemical precipitation, ion exchange, filtering, electrolysis, reverse infiltration, condensation, and adsorption, have been employed to remove heavy metals from contaminated water [5].

Chemical precipitation produces enormous sludges but is characterized by straightforward processes, low prices, and simple automatic pH control. The electrolysis method is characterized by a decrease in sludge generation, a metal hydroxide that clogs the membrane but does not require chemical treatments [21]. Ion exchange produces less sludge but offers the advantages of selectivity, affordability, and ease of use [22].

Fluctuation is a straightforward technique that is inexpensive, quick to complete, energy-efficient, and has low ongoing costs. The advantages of coagulation-melting technologies include their simplicity, affordability, and lack of sludge. The filtration process is efficient, selective, environmentally friendly, and ineffective, but it also costs money to maintain [23]. Inverse osmosis is an efficient but expensive process that separates metal ions under high pressure using a semi-permeable membrane [22].

1.4 Adsorption Methods For Removing Heavy Metals

In order to remove heavy metals and other contaminants from industrial wastewater, a process known as bioabsorption involves attaching metal ions to the surfaces of abiotic materials like algae, agricultural and industrial waste, microorganisms, biopolymers, etc. Even at low concentrations, contaminants can be removed through biosorption [24] [25].

The biosorption process is created by a variety of mechanisms, including filtering, the physico-chemical reaction, and the precipitation of metallic ions, and it comprises a solid phase (biomass) and a liquid phase (water). This method is affordable, effective, simple to use, and generates little sludge [24]. Whether a functional group is present on the biomass surface affects the biosorption process [26].

A layer of metal ions formed on the surface of the adsorbent material as a result of the accumulation of liquid, gaseous, or solid atoms or ions during adsorption. It is commonly utilized in industrial applications such as activated charcoal, synthetic resins, and water purification because of its effectiveness at removing pollutants and its low cost. Adsorption is thought to be useful for cleaning up contaminated water because it is straightforward and efficient [5] [10].

Absorption is absorbed by physical means when the interaction of adsorption through Van der Waals is fully combed into the table. This is because the sub-absorption and adsorption of weak bonds are formed in the actual adsorption process, which makes it possible to create and destroy adsorption bonds. On the other hand, adsorption through chemical interactions between adsorption species and adsorption schedules is called chemical adsorption. The chemical adsorption procedure is generally irreversible and slow, as it requires a strong link between adsorption and adsorption and can alter the adsorption surface and chemical properties [27].

1.5 Application of Natural Polymers used In Waste Water Purification

A polymer is a big molecule made up of recurring structural elements. Usually, covalent chemical connections are used to join these subunits. The use of natural polymers for pharmaceutical purposes is appealing due to their availability, lack of toxicity, and affordability. Both synthetic and natural polymers are available. With a few exceptions, they are also biocompatible, potentially biodegradable, and chemically modifiable. Pharmaceutical formulations specifically utilize plant-derived polymers in the production of solid monolithic matrix systems, implants, films, beads, microparticles, nanoparticles, inhalable and injectable systems, as well as viscous liquid formulations [28]. On the other hand, industries like metal plating, excavation, and battery production have emerged as a result of industrialization. The chemical industry uses a variety of toxic, mutagenic, carcinogenic, or essentially non-biodegradable materials. Wastewater typically has a range of organic and inorganic material concentrations [3] [29].

Since highly toxic chemicals are released from more than 80% of harmful waste sites, water contamination is to blame as the main factor contributing to the decline in human health. Bio-nanocomposites have been widely used in the past few decades in both academic and industrial settings to address a variety of water purification issues [30]. The process of purifying water involves removing harmful elements such as microorganisms, organic materials, suspended and colloidal particles, and suspended and colloidal particles. Minerals, chemical molecules, and gases make up dissolved impurities, which change the physical properties of substances (temperature, turbidity, color, alkalinity, pH).

Since they are the result of chemical interactions between water and other things, solubilizing pure water is not a property that occurs naturally [31].

The traditional methods for treating oily wastewater have included chemical precipitation, ion exchange, filtering, electrolysis, reverse infiltration, condensation, and adsorption, which have been employed to remove heavy metals from contaminated water [5].

One important component of natural polymers is a lignocellulosic waste. cellulose (40–50%), hemicelluloses (25–30%), and lignin (15–20%) are the three primary components of this [32].

1.5.1 Cellulose

The molecular name for cellulose is (C6H10O5) n, and it is an organic polysaccharide made up of a linear chain of several hundred to more than ten thousand linked glucose units. Several parallel cellulose molecules combine to create crystalline microfibrils, which are robust and immune to enzyme attack [28].

The primary polysaccharide in lignocellulosic materials, which consists of a few hundred to over ten thousand 1,4-connected D-glucose units in unbranched linear chains, is called cellulose. These are referred to as microfibrils and have a width of 3-5 nm and a length of many micrometers [32].

Figure 1.1
Structure of Cellulose

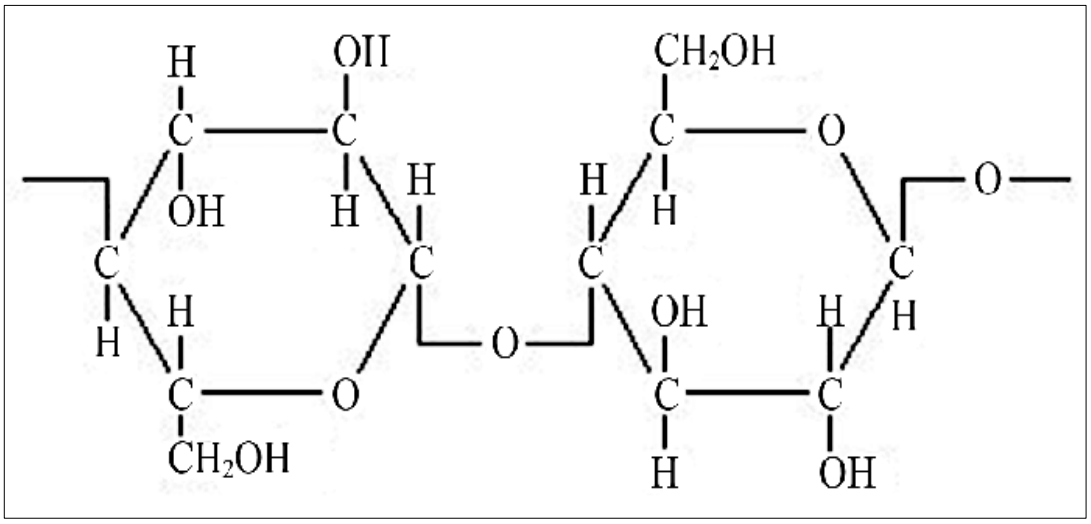

Together with cellulose and lignin, hemicellulose is arranged as closely knit strips. Pentose, hexose, glucose, mannose, and galactose are all found in branching heterogenous polysaccharides in this substance [32].

The material qualities of cellulose are intriguing, including strong force, superior mechanical estate low density, affordability, and good biocompatibility [33].

1.5.1.1 Recent Work Using Cellulose

Cellulose is a big, linear-chain polymer containing a lot of hydroxyl groups [34]. The name "β-1,4-glucan" refers to the acetal functionalities between the equatorial OH group on the carbon atom (C4) and carbon atom (C1) that covalently link the repeat units of β-D-glucopyranose in cellulose [35].

Cellulose beads can be altered to produce cellulose-based adsorbents that can be used in the production of bio-based goods like adhesives and coatings. It is inexpensive, non-toxic, and biodegradable to use the natural, renewable polymer cellulose [36].

Numerous modified cellulose adsorbents demonstrated renewability and reusability over a number of adsorption/desorption cycles, enabling recovery of the adsorbed heavy metal in a more concentrated form. The ability of unaltered cellulose to bind heavy metals is modest, and its physical stability is inconsistent. In order to provide acceptable structural durability and a highly effective capacity for the adsorption of heavy metal ions, chemical modification of cellulose can be carried out. According to a study, the structure of cellulose modified citric acid can remove 21.64 mg/g Pb(II), 18.06 mg/g Cu(II), 8.36 mg/g Zn(II), and 42.69 mg/g Cd(II) of heavy metals. The heavy metals adsorption utilizing modified nanocellulose materials was

86.47% Pb(II), 77.40% Cu(II), 70.04% Zn(II), and 85.20% Cd(II) in contrast to the % adsorption using the structure of cellulose modified citric acid of less than 5% [37]. These findings led to the conclusion that the structure of cellulose modified citric acid might be employed as a low-cost adsorbent for the removal of heavy metals and that it could be used to construct household water filtration systems [38]. Another study used the new welan gum- structure of cellulose modified citric acid as an adsorbent to bind Cd(II), Pb(II), and Cu(II) ions. The adsorbent was created through emulsification, regeneration, and modification, and its maximum adsorption capacities were 83.6, 77.0, and 67.4 mg/g, respectively. Additionally, as the temperature rose, the three metal ions' adsorption capabilities increased. The largest amount of adsorption takes place at pH 5 [35].

A study found that the amidoximated grafted structure of cellulose modified citric acid has a high capacity to adsorb metal ions from aqueous solutions, with capacities of up to 1.7 mmol/g for Co(II), 1.6 mmol/g for Cu(II), and 0.84 mmol/g for Ni(II) ions, respectively [39]. A different study makes use of the structure of cellulose modified citric

acid /chitosan (chitin) composites as biodegradable biosorbents made with ionic liquids. The results showed that the highest adsorption capacity and best stability among the produced biosorbents. At the same initial concentration of 5 mmol L1, the capacity of adsorption was determined to be Cu(II) (0.417 mmol/g) > Zn(II) (0.303 mmol/g) > Cr(VI) (0.251 mmol/g) > Ni(II) (0.225 mmol/g) > Pb(II) (0.127 mmol/g) [40].

A very similar work utilizing the mercerized structure of cellulose modified citric acid was carried out. Results showed that the quantities of heavy metals adsorbed for Cu(II), Cd(II), and Pb(II) were 30.4, 86, and 205.9 mg/g, respectively [41]. In another study, rice hull and sawdust, two structure of cellulose modified citric acid -based materials, were utilized to adsorb heavy metals, such as Pb(II), Cu(II), Cd(II), Zn(II), and Ni(II), from artificial solutions and wastewater samples. Compared to sawdust, rice husk demonstrated a better ability for adsorption. The outcomes demonstrated that the alkali treatment had the greatest capacity for adsorption (alkali > heat > non-modified > acid) [42]. The removal of Ni(II), Cu(II), and Cd(II) ions from aqueous solution was accomplished by the graft copolymerization of aminopropyl triethoxysilane, and the maximum adsorption capacities for these ions of the modified adsorbent were 2.734, 3.150, and 4.195 mmol/g, respectively [43]. Another investigation revealed that the structure of nano cellulose fibers modified citric acid improved sorption efficiency (more than 90%) and stability in terms of increased (3 to 5) regeneration cycles for Cd (II), Pb (II), Ni (II), and Cr (III) ions in single and multi-metal solutions [44].

1.5.2 Hemicellulose

As a naturally occurring polysaccharide, hemicellulose is the second most prevalent element in plant materials. It makes up between 20% and 30% of the total weight of the lignocellulosic biomass and has a weak, random structure [45]. It is believed that hydrogen bonds and Van der Waal interactions help hemicellulose cling to cellulose in plant cell walls.

In order to produce lignocellulosic biomass, plants can combine cellulose to construct extremely durable networks [46].

Figure 1.2
Structure of Hemicellulose

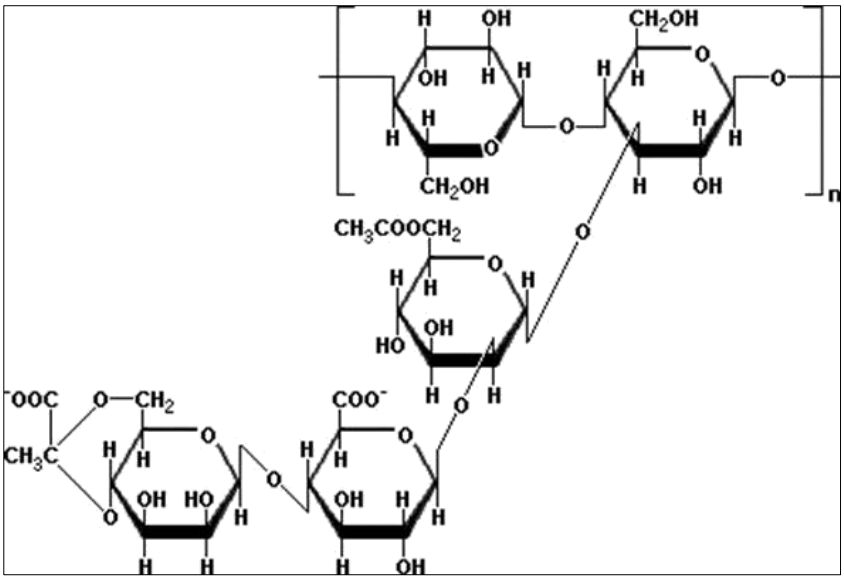

Hemicellulose can be found in a wide variety of plants, at different molecular and structural levels, in many different plant sources and habitats [47].

Hemicellulose is obtained from many plant sources and plant locations with various molecular and structural types [47]. This biomass resource is environmentally benign, biodegradable, and has unique physical and chemical properties. It is anticipated that it will be used extensively in the packaging, food, pharmaceutical, biomedical, cosmetic, textile, and papermaking industries [48].

1.5.2.1 Recent Work Using Hemicellulose

Hemicellulose has been widely employed as an adsorbent to remove dangerous substances from wastewater.

A study found that hemicellulose adsorption significantly enhanced pulp beatability. By adsorbing hemicelluloses onto pulp, it was possible to significantly boost the pulp's physical strength when compared to traditional Kraft pulp. For comparing pulp tear strength at a specific tensile level, a 20–25% increase in tensile strength and an 8–10% increase in tear strength were noted for both hardwood and softwood pulps. [49].

According to a different study, hemicellulose-based hydrogels may be useful adsorbents for removing methylene blue from wastewater. These hydrogels had maximum adsorption capacities of 148.8 and 95.6 mg/g of methylene blue, respectively [50].

In another study, the structure of hemicellulose modified citric acid adsorption could provide a noticeable increase in the physical strength of the pulp. Both hardwood and softwood pulps showed an up to 25% improvement in tensile strength. When evaluating pulp rip strength at a specific tensile threshold, adsorbed pulp showed a somewhat greater bulk property [49].

A study found that the structure of hemicellulose chitosan modified citric acid foam biosorbent uptakes Pb (II), Cu (II), and Ni (II) ions from the aqueous medium at initial concentrations at pH 5 at rates of 2.90, 0.95, and 1.37 mg/g, respectively [51]. By extracting the structure of hemicellulose modified citric acid from barley straw, a study found that the Pb (II) adsorption capacity was attained at pH = 5, 0.4 g/L adsorbent dosage, 55 °C temperature, and 277.78 mg/g, and the removal efficiency was over 99%. Additionally, after five reuse cycles, considerable lead absorptivity was observed [52].

An investigation found that the maximum adsorption capacities of Pb (II), Cd (II), and Zn (II) were 859, 495, and 274 mg/g, respectively. A hydrogel with high xylan content and g-AA demonstrated outstanding metal ion recovery and regeneration properties [53]. Ferrari and colleagues created a brand-new structure of hemicellulose – based hydrogel modified citric acid. The as-prepared hydrogels have adsorption capacities of 635, 448, and 158 mg/g for Pb (II), Cd (II), and Zn (II), respectively. While the adsorption capacity considerably increased when the pH value climbed due to the base's proton depriving action [54].

Lignin is the one polymer that have been used in water purification, its present in olive industry liquid waste.

1.5.3 Lignin

1.5.3.1 Lignin Structure and Properties

lignin is the second most common natural polymer in the world after cellulose. It is a naturally occurring polymer containing aromatic subunits that is present in thicker (secondary) cells and is a significant waste result of agricultural waste. For strength, stability, and defense against biological and chemical attackers, this structure in the plant cells creates a specific matrix [55] [56].

A plant's biomass is made up of 16 to 33% lignin. Due to its limited biodegradability and intricate chemical connections that connect its monomers, lignin is the most prevalent and complicated biopolymer in the world. Radical polymerization of various polymers is used to create the phenyl-propane units that make up this substance. Over 5.0 ×105 tons of it are produced annually all over the world. Industrial lignin is frequently produced as a by-product or waste during the pulping and biofuel production process [57].

Native lignin has limited metal ion adsorption capabilities and a propensity to agglomerate in solvents. Nano lignin, on the other hand, performs significantly better thanks to its enhanced surface area. Delignification and purification procedures were needed to separate lignin from cellulose because of the lignin's potent bonding ability with the latter [36].

Figure (1) illustrates how it is joined to cellulose and hemicelluloses inside the lignocellulosic matrix (1). It is distinguished by its affordability, accessibility, stabilizer, antioxidant, biodegradability, and renewable nature [55] [58].

Figure 1.3

The position of lignin within the lignocellulosic matrix

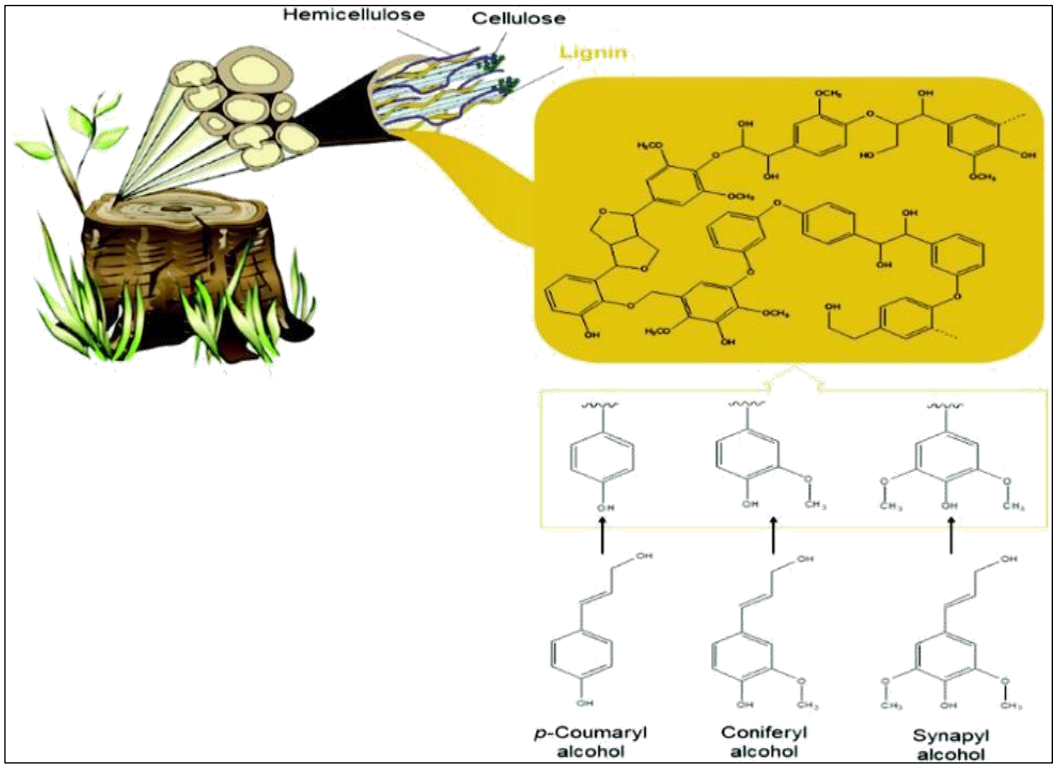

The second-most abundant source of carbon in nature, lignin serves as a raw material for useful chemicals and fuels, substituting fossil fuels and reducing carbon dioxide emissions. It is a potential source for phenol compounds since it is thought to be a macromolecule with alkyl phenol units [59] [60].

Three different types of phenylpropane units make up the aromatic three-dimensional polymer known as lignin. Due to its large surface area, it may absorb a wide variety of heavy metal ions. New lignin-based adsorbent materials have been created in large quantities [57].

Figure 1.4

Chemical structures of the phenol precursors

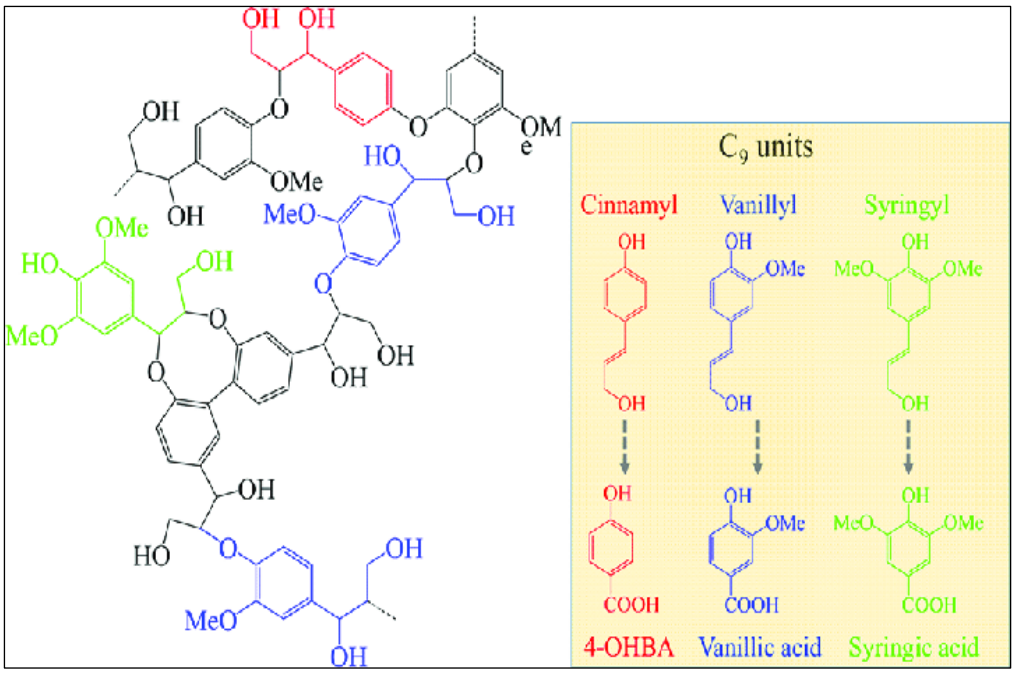

Source: 1- Rinaldi, R., Jastrzebski, R., Clough, M.T., Ralph, J., Kennema, M., Bruijnincx, P.C.A., Weckhuysen, B.M. (2016).
2- Ragauskas, A.J., Beckham, G.T., Biddy, M.J., Chandra, R., Chen, F., Davis, M.F., Davison, B.H., Dixon, R.A., Gilna, P., Keller, M. Langan, P. Naskar, A.K., Saddler, J.N. Tschaplinski, T.J., Tuskan, G.A., Wyman, C.E. (2014).

Figure 1.5

Chemical structures of lignin and building blocks

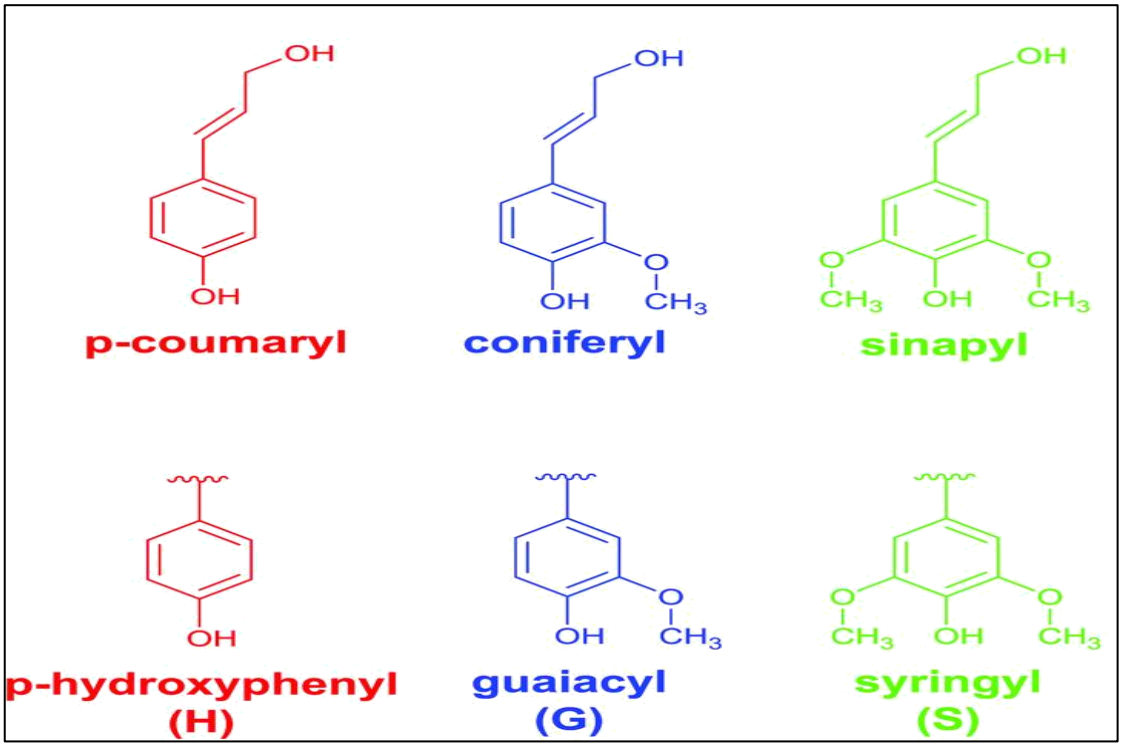

Since the lignin polymer is made up of three-dimensional units connected by ether-carbon bonds, it is extremely resistant to chemical and biological breakdowns [63].

Acidic sites like carboxylic and phenolic sites on the surface of lignin have the ability to effectively absorb heavy metals [64].

According to Ralph et al. (2004) [65], the lignin structure has a variety of linkages, including ether-type bonds (C-O-C) and condensed-type bonds (C-C) as shown in Figure (3). The main connections that make up lignin's structural units are β-O-4 (β-aryl ether), (resinol), and -5 (phenylcoumaran), and these connections influence how reactive lignin is [56]

Figure 1.6
Possible linkages between lignin building blocks

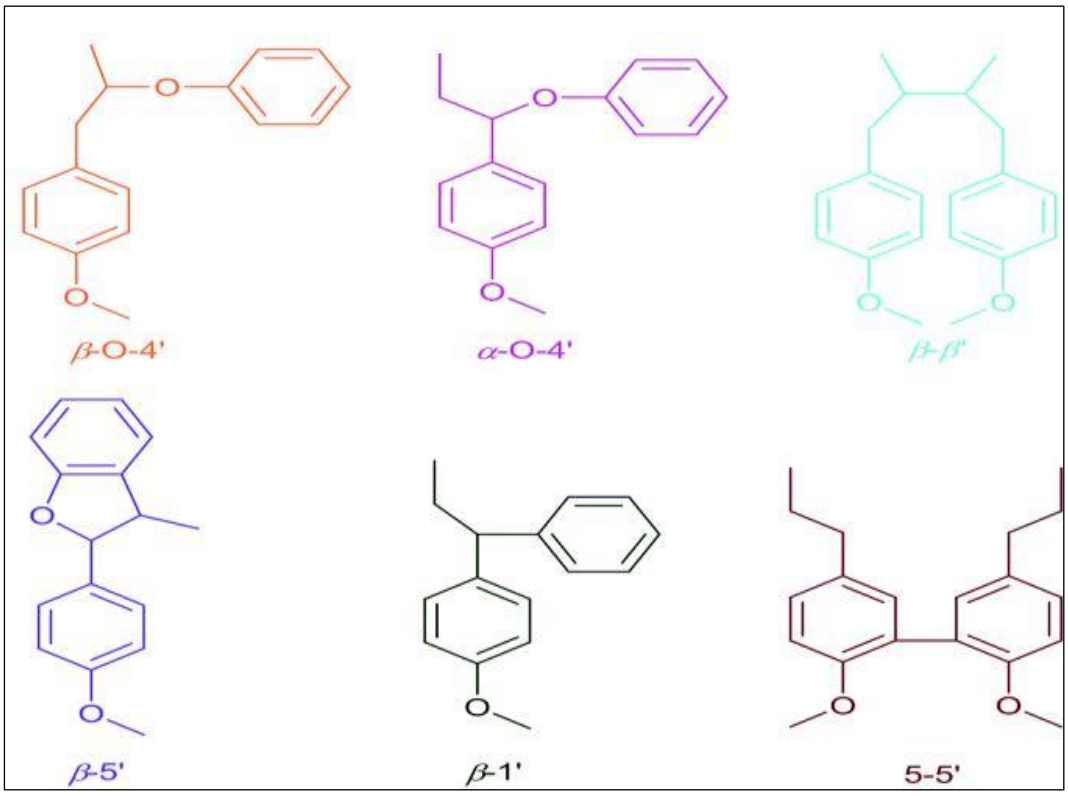

It has been calculated that up to 80% of the bonding motifs present in lignin are represented by the β-aryl ether (or β -O-4) linkage [65] [66]. Therefore, by severing the ether and condensed-type linkage between the lignin units, phenol may be extracted from lignin. Functional groups such as methoxyl, benzyl alcohol, phenolic and aliphatic hydroxyl, noncyclic benzyl ether, carboxyl, and carbonyl groups, etc. are another aspect that affects the interaction [56]. The primary pendant group in the alkyl phenol units is the methoxy group (OCH3) [67].

There are several methods for lignin hydrolysis into phenol compounds that have been reported, including pyrolysis [68] [69], catalytic pyrolysis [70] [71], alkaline oxidation [72][73], hydrolysis [74][75]. Because a solid catalyst may be used in the catalytic process, which is particularly effective for extracting phenol chemicals from lignin and is simple to separate from the reaction's solvent and byproducts, the catalyst is a key component.

1.5.3.2 Lignin Peroxidase

Heme-containing enzymes known as lignin peroxidases (LiPs) break down lignin and its byproducts when H_2O_2 is present. The monomeric glycosylated enzyme LiPs has a molecular weight range of 40−68 kDa, four carbohydrates, 343 amino acid residues, two calcium ions, and a heme group, two calcium ions, 343 amino acid residues, 370 water molecules, and 4 carbohydrates [32] [76].

(LiP) has the ability to oxidize a variety of aromatic organic compounds with redox potentials higher than 1.4V by one electron. In the presence of co-substitutes such H_2O_2 and veratryl alcohol, LiPs are also capable of breaking down lignin another phenolic compound [32].

The first ligninolytic enzyme to be isolated from Phanerochaetechrysosporium was lignin peroxidase (LiP), which was discovered to possess a heme cofactor capable of oxidizing extremely high potential sites, such as aromatic rings [74] [77].

In addition to lignin peroxidase, fungi also secrete heme-containing manganese peroxidases (MnP) [78] [79], versatile peroxidases (VP) [80], as well as multicopper-dependent laccases, which are used to break down lignin.

A number of other bacteria, including Actinomycetes like Streptomyces viridosporus, strains of Nocardia, and Pseudomonas, are also known to break down lignin. Phenylpropanoid dimers, the initial breakdown products, were converted to phenol monomers via aromatic meta-cleavage

pathways by soil bacteria such as Sphingomonas and Pseudomonas, as shown in Figures (6) and (7) [8].

Figure 1.7

The initial breakdown products lignin by Streptomyces viridosporus

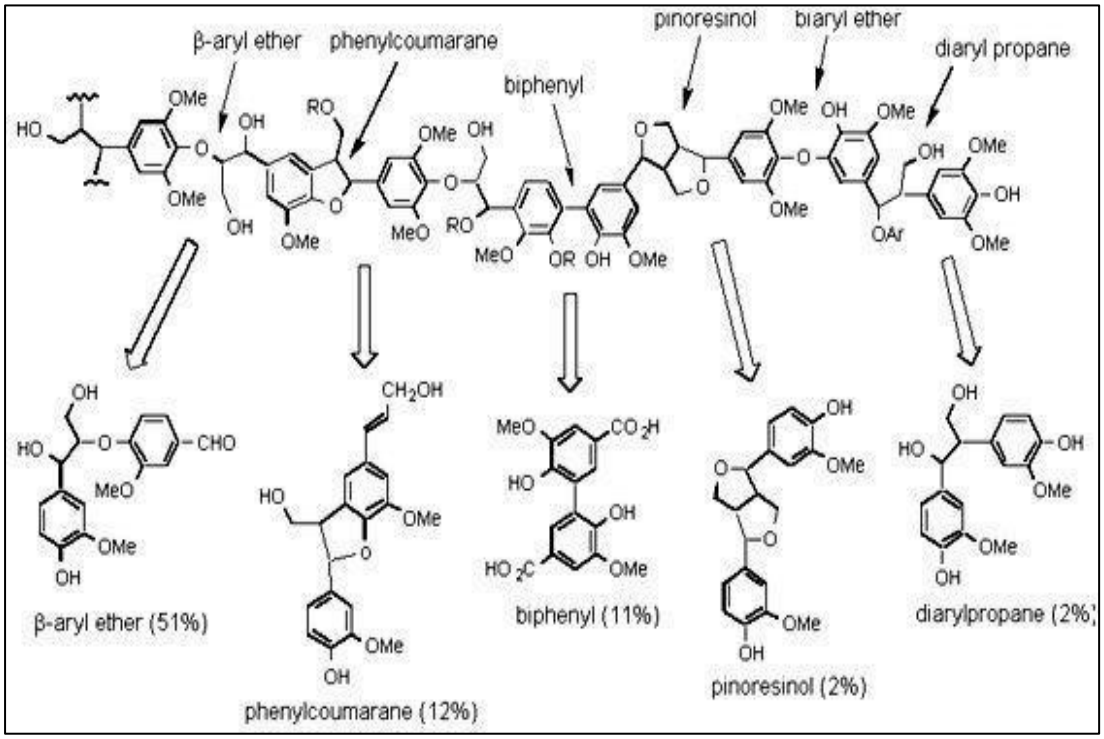

Figure 1.8

Phenylpropanoid dimers (degradation) to phenol monomers by soil bacteria

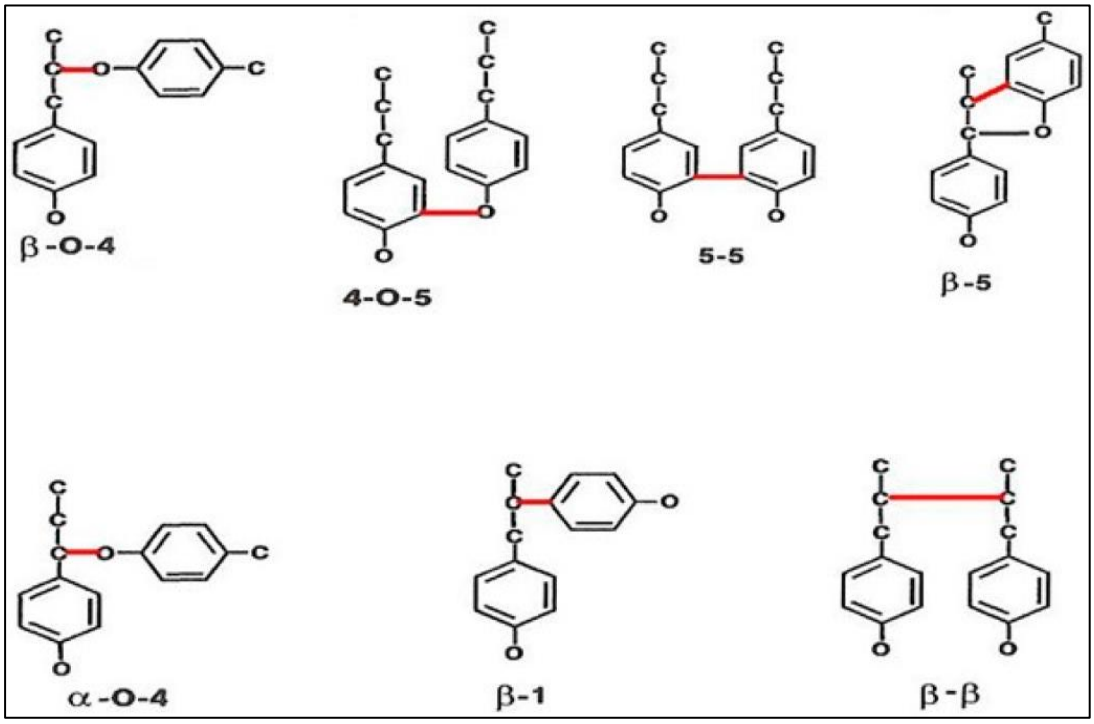

The effectiveness of the enzymatic degradation strategy for converting the lignin found in OILW to phenols will be assessed in this paper.

1.5.3.3 The Catalytic Cycle

When the C-O or C-C connections of bonds between the lignin units are broken to produce phenol, depolymerization reactions are utilized to transform the lignin into different products. Hydroprocessing or oxidation is used to finish the lignin conversion [56]

A typical catalyst is present in lignin peroxidase (LiP). These bacteria that are required for hydrolysis create the enzyme. LiP may break down several phenolic compounds, including lignin, when H_2O_2 is present as a co-substrate and mediators such as veratryl alcohol (VA) are present [81].

The degradation catalytic cycle involves:

Step 1: Two-electron oxidation of the resting (native) ferric enzyme ([LiP]-Fe(III)) by H2O2 to form the oxo-ferryl intermediate [Fe(IV)];

Step 2: Reduction of the oxo-ferryl intermediate [Fe(IV)] by the non-phenolic aromatic reducing substrate (A) to form intermediate II by gaining one electron;

Step 3: Finally, the oxidation cycle ends when intermediate II is returned to the resting ferric state with a gain of one more electron from the reducing substrate (lignin). A sketch of the catalytic cycle is shown in Figure (8).

Figure 1.9
Catalytic cycle for the degradation of lignin using lipase

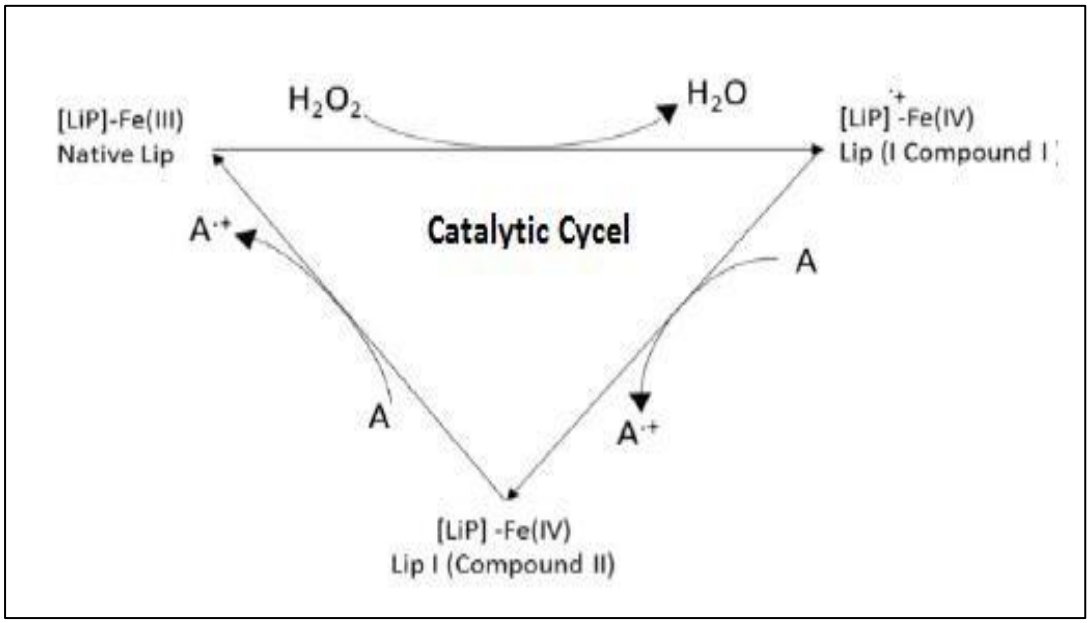

This method uses acidification or column chromatography to remove lignin from an OILW sample. The effectiveness of the enzyme toward lignin breakdown will be assessed as a function

of temperature, time, enzyme dose, and lignin concertation after the extracted lignin is treated with peroxidase enzymes (hem and lignin) in the presence of hydrogen peroxide as a promotor. TLC, UV spectroscopy, and GC/MS will all be used to keep an eye on the degradation process.

1.5.3.4 Recent Work Using Lignin

Alkaline boiling of wheat straw yielded a structure of lignin modified citric acid, which Todorciuc et al. [82] observed had a saturation adsorption quantity for Cu(II) in the water of 26 mg/g. By using sodium alginate and epichlorohydrin to cross-link [82]. Li et al. [56] created lignosulfonate spheres. At pH 5.0 and 30 °C, the spheres showed 27.1 mg/g Pb(II) adsorption, according to batchwise adsorption studies. A monolayer coverage adsorption was indicated by the adsorption behavior, which followed the intraparticle diffusion equation and the Langmuir equation. The continuous removal of Pb(II) from wastewater might likewise be accomplished by packing these spheres in a column [56]. Research showed that the H_3PO_4-activated lignin has a low maximum adsorption value of 29.1 mg/g for Cr, [83]. According to Merdy et al. [84] structure of lignin modified citric acid

hydrolyzed from wheat straw had a low capacity for adsorbing Cu(II) at 20 °C (4 mg/g), but Ca(II) had no effect on the efficacy of the adsorption Merdy et al. (2002) [84]. Acemioglu et al. [85] found that the ethanol-based organosolv structure of lignin modified citric acid had a 1.68 mg/g adsorption capacity for Cu(II) at 20 °C, which is a very low value. The Freundlich equation provided an accurate description of the adsorption process and revealed the heterogeneity of the structure of lignin modified citric acid surface. The structure of alkaline lignin modified citric acid from beech and poplar woods were reported by Demirbas [86] for the adsorption of Pb(II) and Cd(II), with saturation adsorption levels of 9.0 and 7.5 mg/g, respectively. For the adsorption of Pb(II) and Cd(II), Demirbas [86] reported using the structure of alkaline lignin modified citric acid that were isolated from beech and poplar woods, with saturation adsorption levels of 9.0 and 8.0, respectively (Demirbas, 2004) [86].

In a different investigation, it was shown that increasing the reactions between the three phenylpropane units in the structure of lignin modified citric acid for β-O-4and C-C connections at 450 °C and 5 MPa pressure led to the highest phenolics (70.4%) and phenol (42.6%) contents. Methoxyphenol experienced rapid secondary monomolecular dissociation processes under pyrolysis pressure to create phenol and alkyl-phenol [87]. Another study showed that the yield of 4-vinyl phenol increased by almost five times and reached 4.89 weight percent at 600 °C.

Removing hydrogen from the amino increases the pyrolysis process' ability to cleave the Cβ-O link [88]. Aresearch focused on creating eco-friendly comthe posite from the structure of lignin modified citric acid (eethyleneimine. The outcomes showed that at pH 6.0 and 25 °C, the highest adsorption capacities for Cu(II), Zn(II), and Ni(II) were 98.0 mg/g, 78.0 mg/g, and 67.0 mg/g, respectively [89]. Another study created a composite using graft-polymerized bentonite/sodium lignosulfonate, acrylamide, and maleic anhydride hydrogel (BLPAMA).

The saturated adsorption quantity toward Pb(II) was 314.8 mg/g at pH 5.0 and 25 °C, indicating that the adsorption process of lead ions by BLPAMA was temperature-independent but substantially pH-dependent. The Langmuir equation was followed by the adsorption isotherms and the pseudo-second-order equation by the Pb(II) adsorption kinetics, suggesting monolayer chemical adsorption [57]. When incubated at pH 3.5 or

55°C, the activity of the manganese peroxidase (MnP) generated by the linguini-degrading white-rot fungus Echinodontium taxodii 2538 peaked, but it can continue to exhibit high enzyme activity after 24 hours at pH (2.0-6.0) and temperature (less than 45°C) [90]. With ABTS as the substrate, EtL2538, a white-rot fungus that breaks down lignin, demonstrated its optimal pH at 3.0 and its ideal temperature at 60 °C. EtL2538 showed increased thermostability and maintained more than 80% of its initial activity following a two-hour incubation at 50 °C [91].

1.6 Olive Industry Waste (OIW)

Olive mill waste (OMW) is an organic suspension primarily composed of 80-92% water and 3– 15% organic substances. Due to their toxic nature toward plants and soil microbes, phenolic compounds are regarded to be the waste that does the greatest harm [92].

Nearly 50% of the West Bank's arable land is occupied by olive groves, and oil production provides around 28.7% of the region's total domestic agricultural income. There are both contemporary and conventional types of olive mills. It goes without saying that olive mills are typically located adjacent to olive groves [93].

The olive oil industry is one of the most important agro-food sectors in the Mediterranean and Middle East, including Palestine. For example, according to the Palestinian Ministry of Agriculture, approximately 135,000 metric tons of olives are produced annually in the West Bank and Jordan [93].

Two basic techniques are used to extract olive oil: traditional (classical pressing) and continuous (centrifuging). The oil is separated from the liquid mixer in the traditional technique after the olives are pressed in bags and rested in a series of tanks or using a centrifuge. The large organic load and high concentration of phytotoxic and antibacterial phenolic compounds in the olive waste make it a significant pollutant. Before being disposed of in wastewater treatment plants, it has traditionally undergone detoxification. With the recovery of usable byproducts, olive waste is currently being used more and more [94].

The olive-mills produce massive quantities of waste during the short olive harvesting season (October to January) and are required for oil extraction operations that use a lot of water (Zibar). Overall, olive mill waste accounts for about 44 % of the solid waste of the

olive industry locally known as Jeft, and 56 % of the liquid waste of olive factories locally known as Zibar [93].

These wastes are acid wastes and, with the exception of high biological oxygen demand (BOD) and chemical oxygen demand (COD) values [95].

Waste materials pose challenges to the waste management of olive mills, as well as concerns for environmental scientists, as they cause serious disposal problems [96]. The size and magnitude of olive production worldwide mean that a large amount of untapped agricultural waste is generated, thus creating serious environmental problems in the region.

Unchecked OMW disposal on soil reduces water retention and infiltration, raises soil hydrophobicity, and has significant phytotoxic and antimicrobial effects. It also has an impact on microbial activity, lipid content, organic acids, nitrogen immobilization, nutrient leakage, salinity, and acidity of the soil [92].

1.6.1 Olive Industry Solid Waste (OISW)

Olive mill solid waste (OMSW) is a form of olive cake made in Palestine using pressing procedures. It contains crushed olive kernel shell fragments, skin, and pulp. OMSW can be turned into valuable resources for the production of fertilizer, animal feed, and energy for farmers [97].

OISW is used as an absorbent material to remove water pollutants because it contains different functional groups like phenolic groups, carboxyl, and hydroxyl, which work to remove pollutants from polluted water and treat it. OISW is considered smelly because it contains volatile fatty acids, is a renewable resource, and is used in environmental technology to treat sewage [98].

Olive mill waste (OMSW) is difficult to handle on a big scale and is a significant cause of environmental pollution in its unprocessed state. Although OMSW has the potential to be a useful renewable energy source, storing and disposing of it when it isn't in use adds to storage and disposal costs [97].

OISW has high humidity and oxygen content, which reduces the value of heating while posing environmental problems such as corrosion, sedimentation, and pollutant

emissions. Additionally, chlorine levels that are beyond the allowable limits (more than 0.70% in the pulp portion) cause soil acidification and plant poisoning. In addition to harmful compounds, burning solid waste produces them [99].

OISW is primarily composed of lignin and cellulose, which provide the soil with carbon and nitrates. However, because it contains 98% phenol, it cannot be applied directly to the soil; instead, it is used in the fertilizer industry as green waste [100].

This biomass lowers CO_2 emissions and is a source of sustainable energy. Many carcinogens and hazardous compounds, such as tar, organic carbon particles, and organic acids, are produced when solid waste is improperly disposed of, such as during combustion [101].

1.6.2 Olive Industry Liquid Waste (OILW)

The by-product of processing olive fruit is called olive mill liquid waste (OILW). OMW has a black or reddish black color because of phenolic chemicals, a potent odor, and a high percentage of fat, oil, and grease in addition to lignin is what gives the effluents their dark brown color [102].

Three phases are produced by the most typical extraction method: an oily phase, a solid residue, and an aqueous phase. OMW generally has a pH of 4-5, and a high concentration of polyphenols.

It offers a lot of benefits, including high electrical conductivity, a lot of polyphenols and aromatic compounds, and high (COD) and (BOD) levels [103]

Wastewater from the several olive mills is dumped into the wadies. The resultant high organic pollution in the wastewater has an impact on the soil, groundwater aquifers, waterways, and the ecosystem [96]. OILW is regarded as a societal issue because it harms plants and microorganisms due to its high salt, phenol, heavy metal, and acidic pH content [104].

Since OILW contains both water and organic compounds, it is processed and transformed into soil fertilizer because it cannot be applied directly to soil or crops due to its harmful effects on plants [105]. By adding more organic matter and essential nutrients to the soil, OILW and pomace may boost land yield (potassium, phosphate, and nitrogen). This is

significant because the bulk of agricultural soils in the Mediterranean region is deficient in organic matter and soil nutrients [92]

The region's consumption of OILW has increased as a result of the growth in the number of olive groves. OILW's caustic nature and high concentration of suspended solids make it completely illegal to discharge it into the municipal sewer system [92].

Disposing of the OILW wastewater reduces the economic worth of the olive industry. The economic viability of wastewater disposal using centralized waste-to-energy plants has been assessed under the presumption that wastewater treatment is required prior to disposal. The OILW, on the other hand, is typically disposed of through the sewage system or uncontrolled release above ground, which has detrimental effects on animals as well as the quality of surface and subsurface water. OILW is a significant issue for an industrialist as a result of the ever-rising environmental demands.

Finding an economically viable and environmentally friendly way to turn waste from the olive industry into useful products is the problem. As a result, to solve this issue, the liquid waste from the olive industry was chosen for the current study since it is an appealing biomaterial made of hemicelluloses, lignin, and extractives (fatty acids and alcohols). The sum of the three aforementioned components is infinite.

It has been shown in numerous experiments that using lignin as an adsorptive material is highly effective at removing heavy metals from contaminated water. Due to its structural characteristics, such as its high molecular weight and presence of hydroxyl groups, lignin is frequently utilized in adsorption tests to absorb heavy ions [106-110].

Lignin is significant because it fortifies plant cell walls, improves water transport, protects against infections, and delays the microbial rot of wood [111].

As a by-product or waste from the pulping and biofuel manufacturing process, industrial lignin is typically created. Indirect discharge into water resources accounts for about 90–95 percent of industrial lignin. The remainder is primarily burned off as fuel, which depletes natural resources and pollutes the environment [112].

This experiment investigates the effectiveness of ligninolytic enzymes for lignin hydrolysis into phenol during catalytic pyrolysis.

1.6.2.1 Recent Work Using Olive Liquid Waste

A study found that cyclodextrin absorbs methylene blue (MB) through its cavities by the host contacts and that the remaining functional groups affect the adsorption of metal ions and methyl orange (MO) [113].

In the same process, the NTA-CD-CS adsorbent's Hg (II) MB and MO adsorption capabilities were 178.3, 162.6, and 132.5 mg/g, respectively [114]. The sorption of activated carbon-containing poly(-cyclodextrin) is investigated in a study. Results showed the composites to have high removal effectiveness (>75%), good stability, and a pesticide sorption capacity of up to about 50 mg /g1 [115].

A second study found that the optimal conditions for phenol selectivity (95.5%) from unpretreated lignin pyrolysis were a catalyst/lignin ratio of 0.7 at 550°C. Pretreated lignin underwent a considerable increase in phenol concentration (from 0.6 to 7.0 mg/mL) at 50 °C for 60 min [116]. A different study claims that the Fenton catalyst causes the beta-ether bonds connecting the lignin residues to dissolve, which leads to the depolymerization of the lignin. By halting the formation of biochar and lignin condensation, the lignin-iron chelating complex increases the yield of liquid products [117]. One study found that 50.0 grams of lignin could be degraded to produce 4.1 grams of pure phenol.

Additionally, it was shown that the zeolite catalyst adds an OH group to the aromatic ring by hydrolyzing the bonds between aliphatic carbon and oxygen (C-O) and rupturing the Csp2 - Csp3 link in order to remove the propyl structure [118]. The results of the investigation showed that the production of phenolic and hydrogen monomers is enhanced by the presence of charcoal catalysts. Thus, at 650°C, the phenol concentration increased from 15.76 mg/ml to 53.77 mg/ml without the use of a charcoal

catalyst. The content of cresol increased from 20.95 mg/ml to 44.51 mg/ml, however, the concentration of dimethyl phenol decreased from 9.11 mg/ml to 7.76 mg/ml. Up to 85.32 vol.% of hydrogen was found in 45.53 vol.% of the non-catalytic process [119].

1.7 Foam In Waste Water Purification

Foaming is both a phenomenon and a material. In both cases, a gas phase is encased in a dense phase with a spherical shell, easy compressibility, excellent thermal insulation, and low density are the characteristics of polymer foams [119].

The production and diversity of polymeric foams have drastically expanded, becoming an essential component of the yearly polymer production in response to the growing need for lightweight, insulating, shock, and sound absorbing materials. The so-called thermally induced phase separation (TIPS) process, in which the foaming ingredient, which is dissolved in the polymer, produces a phase separation upon heating, followed by nucleation and cell growth, is one of the most frequently used production methods for polymeric foams. In order to create foam, a low boiling organic liquid, such as pentane or hydrochlorofluorocarbons (HCFCs), is typically dissolved into the polymer at concentrations of around 7 weight percent [120].

Two steps are typically required for the foam using the TIPS method. First, a portion of the steam is used to partially foam polymer pellets using a blowing agent. After being put into a mold and being exposed to steam once more, the previously foamed pellets continue to foam. The pellets bond together as a result of the expansion and adopt the mold's shape. Producing substantial blocks of foam material that can be cut into any shape is made reasonably simple by doing this. Additionally, by adjusting the amount of partially foamed pellets fed to the mold, it is simple to adjust the density of the block that is formed [121].

Chapter Two
Experimental

2.1 Basic Experimental

2.1.1 Materials

All of the substances (sulfated ester with 1,4- phenylene diisocyanate, OILW filtrate with hexamethylene diisocyanate, 1,4-Phenylne diisocyanate triethanolamine, ethyl acetate, lead nitrate, copper (II) chloride dihydrate) utilized in this work. Analytical-grade reagents were utilized throughout, and the OILW (Olive Industry Liquid Waste) used in this work was gathered from a Zita Jammain in Jammain village/Nablus, Palestine.

2.1.2 Tools and Procedures

Instruments used in this work include pH meter (model: 3510, JENWAY), balance (Ohaus Crop, item No. AR 3130), water bath shaker (Daihan Lab Tech, 20.00 to 250.00 rpm Digital Speed Control), and mass spectrometer ICP-MS (ELAN 9000, ICE 3xxx C113500021 v1.30) used to measure the concentration of some heavy metals before and after reacting with the prepared polymer.

Thermo Fisher Scientific, Waltham, Massachusetts, USA Nicolet 6700.00 Fourier transform infrared FT-IR Spectrometer outfitted with the Smart Split Peaks Hemi Micro ATR attachment used to record and examine the functional groups of the manufactured polymer. The clever Split Peak is a microsampling accessory for attenuated total reflectance. Diamond ATR crystal is in the accessories. The following criteria were employed: resolution of 4 cm^{-1}, spectral range of 400–4000 cm^{-1}, and scan count of 16 is used. Using a TG/DSC 1 Star System (Mettler-Toledo) coupled with an MS-Thermostar GSD320 (Pfeiffer Vacuum) Mass Spectrometer, measurements of inductively coupled plasma (ICP), thermo gravimetric analyzer (TGA), and differential scanning calorimetry (DSC) were made. TG/DSC curves were measured with Pt crucibles, in N_2 flow (20 mL/min), with Thermal stability, changes in sample composition, and kinetic parameters for chemical reactions in the polymer were measured by TGA under the control of the STAR e software v.10.00 (Mettler Toledo) during the procedure.

Flame Atomic Absorption Spectrometer or FAAS (ICE 3000 series AA System, Thermo Scientific). The amount of residual metal ions present in the solutions under study was calculated using the flame type. At 217 nm, (FAAS used air-C_2H_2). Each analysis test was run in triplicate using an average of three samples, and the findings were presented. The Microsoft Excel application was used to assess the experimental data inaccuracy. The surface topography and nanoscale picture of the polymer surface were determined using AFM equipment from the pharmaceutical department. By placing the sample on mica and utilizing a tapping mode-AFM (core AFM from Nanosurf company, Dyn190Al cantilever, nominal spring constants of 48 N/m), images were produced in the air at ambient temperature. The photographs were analyzed using Gwyddion software.

2.2 Foam preparation

2.2.1 Extracting polyphenol form OILW

A sample of OILW was dried under the hood at room temperature. The residue was used in the following experiments without any further purification.

2.2.2 OILW/ 1,4-hexamethylene diisocyanate (LHMDIC)

After dissolving a sample of 1,6-hexamethylene diisocyanate (10.0 mL, 60.0 mmol) in 20 mL DMF and adding 10 drops of trimethylamine in order to initiate the exothermic reaction, a sample of OILW (10.0 g) was added to the suspension and heated to 60°C. In around 10 minutes, a mound of foam formed. After that, it was left for 60 minutes to guarantee that the reaction was finished, the foam was washed with water and allowed to dry at room temperature. A sample of the prepared foam was ground using Wiley mil as further reference.

2.2.3 OILW/1,4-phenylne diisocyanate (LPDIC)

A 20 mL of DMF was used to dissolve a sample of 1,4-pheneylne Diisocyanate (16.0 g, 100.0 mmol), which was then followed by the addition of 10 drops of triethylamine. In order to initiate the exothermic reaction, a sample of OILW (15.0 g) was added to the suspension and heated to 60°C. Once the reaction had begun, the heat was removed. In around 10 minutes, a mound of foam formed. After being left for 60 minutes to guarantee that the reaction was finished, the foam was washed with water and allowed to dry at

room temperature. A sample of the prepared foam was ground using Wiley mil as further reference.

2.3 Purification of Water Contaminated with Lead using LHMDIC and LPDIC polymers

2.3.1 lead (II) solution preparation

By dissolving 0.1600 g of lead nitrate $Pb(NO_3)_2$ in distilled water and then diluting it to 100 mL in a volumetric flask, a solution with a 1000 ppm concentration was created. From this solution, five standard solutions were prepared, each containing Pb (II) ions in concentrations of 1.0, 5.0, 10.0, 20.0, 30.0, and 50.0 ppm.

2.3.2 Calibration Curves

As shown in Figure 2.4, different concentrations of standard solutions were generated in order to create a calibration curve for Pb(II) ions. The absorbance of the standard solutions was then determined using flame atomic adsorption spectroscopy (FAAS).

Figure 2.1

Calibration curve of Pb (II)

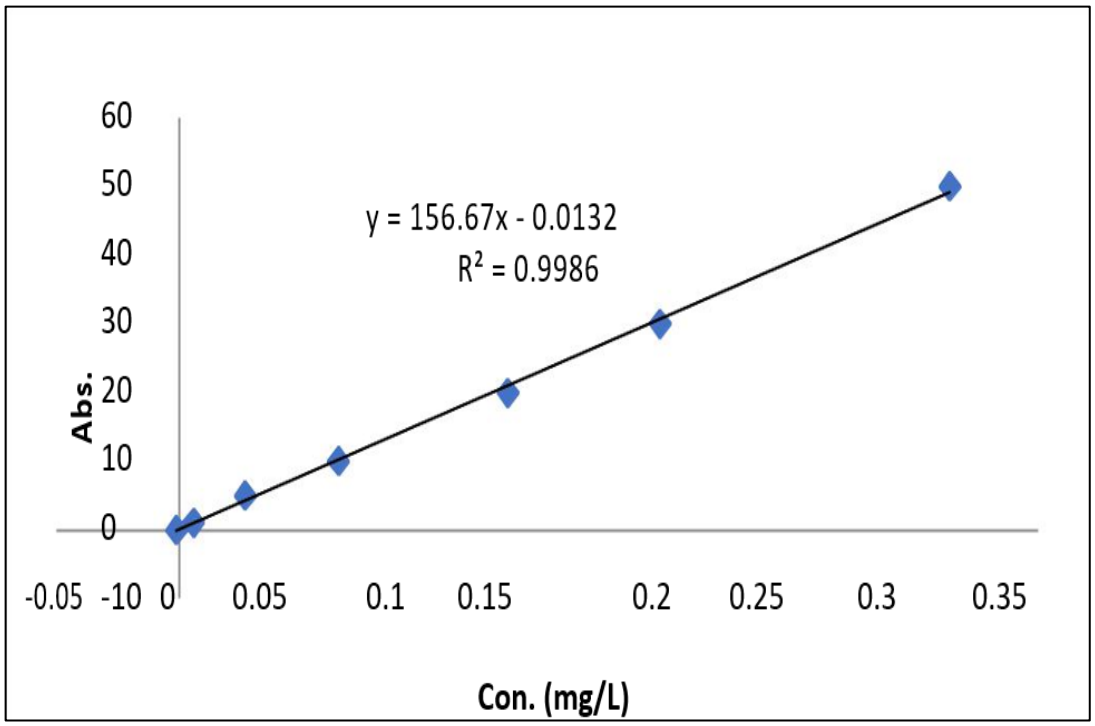

Pb (II) ions calibration curves were plotted using the prepared standard solutions, and the effectiveness of heavy metal removal by LHMDIC and LPDIC polymers adsorption were studied

in relation to the effects of various parameters including pH, temperature, time, initial concentration, and dosage.

Through the use of FAAS (Flame Atomic Absorption) at the wavelength (λ) = 217.00 nm, the adsorption of each and every solution under investigation was quantified.

The residual lead ion concentrations in the filtered samples were determined using the calibration curves for Pb(II) ions, which were used to measure the absorbance of the standard solutions.

2.3.3 Batch Adsorption Extraction Process

In a batch extraction procedure, Pb (II) solution with known concentrations of the LHMDIC and LPDIC polymers were added to bottles, which were then mechanically closed and shaken at a speed of 125.00 periods/min at constant pH and temperature. A sample of each mixture was taken out using a syringe, put through a 0.45 μm syringe filter, and then its residual metal ions concentrations were measured. Atomic absorption spectroscopy, or FAAS, was used to calculate the concentration of lead metals.

2.3.4 Effect of pH

The pH experiment was done to determine the optimum pH values that would allow both the polymer lignin foam with LHMDIC and LPDIC to absorb Pb (II) ions.

A volumetric flask containing 1000 ml of distilled water was used to dissolve 1.6 g of Pb(II). After that, 10 ml was pulled and placed in a volumetric flask of 100 ml, and their pH was adjusted to 3.5, 5.5, 6.5, 8, 11 using 0.5 M HCl and 0.1 M NaOH solutions. 20 ml of sample was placed in another volumetric flask of 100 ml, to prepare a concentration solution of 20 PPM. Standard solutions were prepared from the prior solution with concentrations of (1, 5, 10, 20, 30, and 50 ppm) to make a calibration curve.

The samples were shaken for 30 minutes at 25°C, filtrated by a 0.45 µm syringe filter, and finally analyzed by FAAS. The amount of Pb(II) ions that were absorbed by each polymer are shown in Tables 2.1 and 2.2.

Table 2.1

Effect of pH on the adsorption of Pb(II) from water by LHMDIC

pH	Pb(II)(ppm)	Removal of Pb(II)
3.5	12.54	37%
5.5	0.0094	99.95%
6.5	0.0459	99.77%
8.0	0.02905	98.54%
11.0	1.1065	94.46%

Table 2.2

Effect of pH on the adsorption of Pb(II) by LPDIC

pH	Pb(II)(ppm)	Removal of Pb(II)
3.5	27.37	___
5.5	0.2890	98.55%
6.5	0.5635	97.18%
8	0.2483	98.75%
11	0.8623	95.68%

2.3.5 Effect of polymer dosage on removal effectiveness

This experiment was conducted to determine the maximum amounts of Pb(II) ions that can be removed using LHMDIC at optimum pH 5.5 and LPDIC at the optimum pH 8 form aqueous solutions with a concentration of 20 ppm and volume of 10 .0 mL. Different amounts of each foam (5, 10, 20, 40, and 50 mg) were added to the five solutions. The samples were shaken for 30 minutes at 25°C. The samples were filtrated and analyzed by FAAS to determine the metal ion concentration. The results for both polymers show in Tables2.3 and 2.4

Table 2.3

Effect of adsorbent doses on the adsorption of Pb(II) from water by LHMDIC.

Weight of dose (mg)	Final concentration of Pb (II) (ppm)	Removal of Pb(II)%
5	0.8043	95.97%
10	0.7474	96.26%
20	0.8330	95.83%
40	0.8467	95.77%
50	0.6618	96.69%

Table 2.4

Effect of doses on the adsorption of Pb(II) by LPDIC

Weight of dose (mg)	Final concentration of Pb (II) (ppm)	Removal of Pb(II)%
5	1.1775	76.45%
10	1.4002	86%
20	1.4197	92.9%
40	1.5150	97.1%
50	1.2017	97.6%

2.3.6 Effect of Concentration of Adsorbate

The goal of this experiment was to determine the optimum concentration of Pb(II) ions, which can be removed with the lowest possible adsorbent using the two foams LPDIC and LHMDIC. The adsorption experiment was carried out at pH 8, and adsorbent doses of 20 mg. As previously a solution was prepared of 10 mL with various concertation of Pb(II). All samples were then shaken for 30 minutes at 25°C, microfiltered, and analyzed by FAAS. The results for both polymers are shown in Tables 2.5 and 2.6.

Table 2.5

Effect of concentrations on the adsorption of Pb(II) by LHMDIC

Initial concentration of Pb(II) (ppm)	Final concentration of Pb(II) (ppm)	Removal of Pb(II)%
5	0.9355	81.29%
10	0.6390	93.61%
20	0.4096	97.95%
30	0.4333	98.55%
50	0.4622	99.07%

Table 2. 6

Effect of concentrations on the adsorption of Pb(II) by LPDIC

Initial concentration of Pb(II) (ppm)	Final concentration of Pb(II) (ppm)	Removal of Pb(II)%
5	1.1775	92.99%
10	1.4002	92.9%
20	1.4197	92.42%
30	1.5150	95.77%
50	1.2017	93.99%

2.3.7 Effect of contact time

For both foams, the optimum time to adsorb the greatest quantity of Pb(II) ions was examined. This experiment was performed at the optimal parameters for a 10 mL solution with a pH of 5.5 for LHMDIC polymer and a pH of 8 for LPDIC polymer, adsorbent doses of 20 mg, and a concentration of 20 ppm.

Five bottles each containing 10 ml of 20 ppm solution and 20 mg of each polymer was prepared. Following that, all samples were shaken for varying lengths of time (5, 10, 20, 40, and 60 minutes) at 25°C before being filtered. Finally, these samples were measured by FAAS as shown in Tables 2.7 and 2.8.

Table 2.7

Effect of contact time on the adsorption of Pb(II) by LHMDIC

Time (min)	Final concentration of Pb(II) (ppm)	Removal of Pb(II)%
5	0.6289	96.85%
10	0.9753	95.12%
20	0.8991	95.5%
40	0.8223	95.88%
60	1.0348	94.8%

Table 2.8

Effect of contact time on the adsorption of Pb(II) by LPDIC

Time (min)	Final concentration of Pb(II) (ppm)	Removal of Pb(II)%
5	2.5776	87%
10	2.8181	85.9%
20	3.1739	84.1%
40	3.1289	84.3%
60	3.1929	84.03%

2.3.8 Effect of temperature

This experiment was used to determine the optimum temperature at which the greatest quantity of lead ions could be loaded onto both foams. 20 mg of each foam was added to 10 ml of 20 ppm of Pb(II) solution. Five solutions were prepared they were shaken for the recommended 20 minutes at various temperatures (15 20, 40, and 50^{o}C), the samples were measured by FAAS. The results are shown in Tables 2.9 and 2.10.

Table 2.9

Effect of temperature on the adsorption of Pb (II) by LHMDIC

Temp ^{o}C	Final concentration of Pb(II) (ppm)	Removal of Pb(II)%
5	1.0295	94.85%
10	1.0109	94.95%
20	1.2039	93.98%
40	1.2450	93.77%
60	1.3786	93.07%

Table 2.10

Effect of temperature on the adsorption of Pb (II) by LPDIC

Temp ^{o}C	Final concentration of Pb(II) (ppm)	Removal of Pb(II)%
5	2.2841	88.57%
10	2.0317	89.8%
20	2.6872	86.56%
40	3.1173	84.41%
60	3.1696	84.15%

2.4 Adsorption Isotherm

Adsorption isotherm methods are utilized to explain how the adsorbent will interact with the adsorbate and to comprehend the mechanism of adsorption. For the most part, the observed adsorption processes of heavy metal ions onto inexpensive adsorbents were explained by the Langmuir and Freundlich isotherms models.

2.5 Adsorption Kinetics

To understand the mechanism of the metal ions adsorption process by LHMDIC and LPDIC, the kinetic laws were applied to the findings obtained. The optimal pH, initial concentration, contact time, dose, and temperature, were used to study the adsorption kinetics. Prior to and following adsorption, the metal ion concentration was measured.

Utilizing was used during the experimental portion. The amount of each polymer was added to

10.00 mL of 20.00 ppm of Pb(II) solutions at the optimal parameters of pH 5.5 for LHMDIC polymer and pH of 8 for LPDIC polymer. The mixture was shaken for 5 minutes at 25°C. Measurements of the adsorption rate and comparisons with theoretical models were made. The experimental findings at various contact times were subjected to the first and second order pseudo-kinetic models. The parameters of the pseudo first and pseudo second order kinetic models (K, q_e, and R^2) of the ions adsorption on the foams LHMDIC and LPDIC were established, and the q_e values from calculations and experiments were compared [121].

2.6 Thermodynamic Adsorption

With regard to the thermodynamics of the adsorption process, the temperature is crucial for the adsorption of metal ions. Exothermic or endothermic adsorption processes can often be used to describe the thermodynamic properties of heavy metal adsorption on inexpensive adsorbents.

Adsorption is an exothermic process if it reduces with a temperature increase; alternatively, it is an endothermic process if it increases with a temperature increase. Gibbs free energy (ΔG), enthalpy (ΔH), and entropy (ΔS) are three thermodynamic parameters that are frequently used to analyze the thermodynamic behavior of an adsorption process [10]. The following equations are employed:

$$\Delta G = \Delta H - T\Delta S \qquad \text{Eq. 1}$$

G: the modification of Gibbs free energy (J).

H: the enthalpy change (J)

S: the entropy change (J/K)

T stands for the actual temperature (K).

The following equation relates G to K_d,

the thermodynamic equilibrium constant:

$$\Delta G = -RT\ InK_d \qquad \text{Eq. 2}$$

Where R is the universal gas constant, equaling 8.314 J/.mol.K

K is the thermodynamic equilibrium constant, equaling (q_e/C_e) in mol or (L/g),

and K_d is the constant of thermodynamic equilibrium.

Equation 2 is substituted for equation 1 and rearranged to produce:

$$Ln\ K_d = \frac{\Delta S}{R} - \frac{\Delta H}{RT} \qquad \text{Eq. 3}$$

2.7 Purification of wastewater

A sample of sewage water from a paint industry in (Jericho/Palestine) was collected for this inquiry. To determine the amount of metal present and its concentrations, the sample underwent ICP-AES analysis (the examination was carried out by the Water Center at An-Najah National University, Nablus, Palestine). The effluent was put into three vials, each holding 20 ml. One vial served as a blank; the second contained 50.00 mg of LHMDIC ester the third contained 50 mg of LPDIC. The adsorption was carried out at 10°C for 5 minutes while mechanically shaking the solution at the determined optimal pH of 5.5 for LHMDIC polymer and pH of 8 for LPDIC polymer. The amounts of residual metal ions in each mixture were determined by ICP-AES after a sample was taken from each mixture using a syringe and filtered through a 0.45 μm syringe filter.

Chapter Three
Results and Discussion

In Palestine, the primary agri-food economic activity is the production of olive oil. It produces a significant number of solid and liquid pollutants (such as olive pomace and wastewater from olive mills) that pose a serious environmental issue. As a result, these businesses now face significant difficulty in managing these wastes, which are both detrimental to the environment and abundant in bioactive substances like lignin and polyphenols. From a circular economy standpoint, the recovery of phenolic compounds has been suggested as a clever method for the valorization of these byproducts in recent years. In this work, the fraction of polyphenols and lignin was extracted from OILW and converted to a 3D polymer in the foam form by polymerizing them with polyisocyanate. The foam was used in extracting toxic metal ions from wastewater.

A sample of OILW was dried completely under the hood and extracted with methanol. The methanol solvent was evaporated, and an residue was analyzed by FT-IR. It is composed mainly of phenolic compounds in addition to some low MW lignin and some carbohydrate. The residue components contain hydroxyl groups as shown in Figure 3.1 in appendix b [122] and lignin (Figure 3.2) in appendix b.

3.1 Thermal Gravimetric Analysis (TGA)

TGA was applied for both polymers of the LHMDIC and LPDIC to determine the polymer's thermal stability at high temperatures by measuring the mass of each sample over time as a function of temperature. Results are shown in Figures 3.1 and 3.12

Figure 3.2 demonstrates how the mass of LHMDIC decreases as the temperature rises to 400 °C before stabilizing at 700 °C. When compared to LPDIC, the mass is initially stable but decreases as the temperature rises from 250 °C to 600 °C.
With the temperature rising until it reached 700°C, it resulted in an astonishing 90% mass loss. This result indicates that thermally treated (curing) derivatives OILW are thermally stable.

3.2 FT-IR Experiment

In order to determine the chemical functional groups that are present on both polymers LHMDIC and LPDIC, FTIR spectroscopy was used. wave numbers between 1000 cm^{-1} and 4000 cm^{-1} were used to get IR absorbance data. The main peaks shown in the IR spectrum of LPDIC are 3302, 1634, 1605, and 1216 cm^{-1} corresponding to functional groups N-H, C=O, C=C, and C-N. These peaks prove the formation of the target polyurethane. Figure 3.5 in appendix b shows the following bands 3300, 1637, 1561, and 1216 cm^{-1} corresponding to functional groups N-H, C=O, C-H, and C-N. These peaks prove the formation of the target polyurethane.

FT-IR analysis was also performed on the polymers after metal adsorption. The spectra are shown in Figures 3.5 and 3.6. As shown in the IR spectrum some peaks showed a shift in wavenumber indicating complexation with metal is occurring.

From figure 3.6 in appendix b, There are many peaks appeared in the LPDIC with wastewater adsorption, the peak at 3681.58 cm^{-1} and 3617.55 cm^{-1} were referred to as the O-H stretch. While another peak at 2857.92 cm^{-1} and 1461.62 cm^{-1}were they refer to C-H stretch disappeared. Another two peaks at 2970.59 cm^{-1} and 771.41 cm^{-1}which related to the C-H stretch appeared. The peak at 730.95 cm^{-1} was shifted to 720.92 cm^{-1} and refers to the O-H stretch, also another peak at 3596.68 cm^{-1} was shifted to 3681.58 cm^{-1} which is related to the O-H stretch as shown in figure 3.7. A new peak at 3617.55 cm^{-1} appeared and referred to CH_3 groups. A peak at 3334.47 cm^{-1} was shifted to 3333.90 which is related to the N-H bend. The peak at 2932.33 was shifted to 2970.59 and related to C-H stretch. A new peak at 2932.00 was appeared and referred to O-H stretch, while another peak at 1618.58 which referred to C-N stretch was disappeared.

3.3 Characterization by AFM (Atomic Force Microscope)

Figures 3.9 in appendix b. A show that the derivative OILW's average width, was 30 ± *2* nm, and Figure 3.9.B shows that it was 300 ± 15 nm for OILW that had undergone heat treatment. The size of the pores and the polymer surface changed due to the formation of a new cross-linking chemical bond. It's interesting how thermally processed OILW have a large surface area with a small pore count; the surface almost has a cluster form, which

facilitates the adsorption process. Because of this, the following parts utilized the thermally treated OILW[123]

3.4 Adsorption Outcomes

Using derivative OILW to remove hazardous, heavy metals from industrial effluent is the major goal of this effort. Studying the derivative OILW's propensity for lead Pb(II) ion adsorption was done to carry out this procedure. Equation 3 was used to determine the percentage of elimination after the remaining Pb(II) ion concentrations were examined using a flame atomic absorption spectrometer.

$$\% \text{ adsorption} = (C_i - C_f / C_i) \times 100\% \qquad \text{Eq. 4}$$

Where: C_i stands for the solution's initial concentration of heavy metal ions (ppm).

C_f : Final heavy metal ion concentrations in solution (ppm).

$$q_e = (C_i - C_f / m) * V \qquad \text{Eq. 5}$$

Where V is the solution's volume (in liters)

m is the adsorbent's mass (g).

Equation 2 shows how to compute the equilibrium adsorption capacity qe (mg/g) given a range of ion concentrations in an experiment.

3.4.1 Effect of pH

In this work, the optimal pH for removing Pb (II) ions from water using both polymers of LHMDIC and LPDIC was investigated.

The effectiveness of the adsorption process is significantly influenced by the pH of the solution for Pb (II) solutions, and the impact of pH on the adsorption performance of each polymer was examined. Figure 3.7 in appendix b shows the results for pH values ranging from basic mediums with a pH of 11 to acidic mediums with a pH of 5.5.

As shown in figure 3.10 in appendix b, the highest rate of Pb(II) ion adsorption for LHMDIC polymer was 99.95% at pH 5.5. While for LPDIC, the Pb(II) ion adsorption was at its highest at a pH of 8 which is 98.75%. For both polymers, we observe that as

the pH value increased, adsorption decreased gradually and reached its lowest point at pH = 11.0, due to the negative surface charge on both polymers and increased reactivity with Pb(II) ions as a result of the ionization of their carboxylic groups [112].

3.4.2 Effect of polymer dosage on lead removal effectiveness

By adjusting the doses from 5 to 50 mg for LHMDIC polymer at pH 5.5 and LPDIC at pH = 8, the highest adsorption percentage of Pb (II) ions was investigated. Figure 3.8 illustrate the highest removal of Pb (II) ions for both polymers.

For LHMDIC, the highest adsorption percentage was at 50.00 mg with a removal efficiency of 96.69%. While for LPDIC, at the beginning of the removal process, it reached the lowest value at 20 mg which is 92.42%, because the active sites at the surface were available and empty. After that, the adsorption process increased gradually to the highest adsorption percentage at 40.00 mg with a removal efficiency of 95.77%. The vast number of active sites that are present on the surface of each polymer at its high doses is what causes the significant adsorption of lead ions.

We draw the conclusion from these findings that the change in the adsorption process of the LHMDIC polymer is very slight, and it increases gradually only at the dose of 40.00 mg. While for LPDIC polymer, the Pb(II) ions adsorbed were increased by increasing the dose of LPDIC polymer and the adsorption process intensifies with increasing concentrations of that polymer because it needs a lot of active sites on its surface in order to bind lead ions.

3.4.3 Effect of Initial Concentrations

Both LHMDIC and LPDIC polymers were utilized to evaluate the highest adsorption of Pb (II) ions in the adsorption process at the optimal parameters pH of 5.5 for LHMDIC polymer and pH of 8 for LPDIC polymer, and 50 mg at 25^{o}C. The results shown in figure 3.12 in appendix b over a concentration range from 5-50 ppm.

The percentage of Pb (II) ions removed steadily rises with increasing initial concentrations, as we have observed in figure 3.12, the LHMDIC polymer has a maximum percentage of Pb (II) ions occurring at the concentration of 50 ppm, which is 95.77%, while for LPDIC polymer, the maximum adsorption equal 99.07% at 10 ppm and it continues to be stable after that.

3.4.4 Effect of Contact Time

For each of the polymers LHMDIC and LPDIC, the experiment investigated the optimal period for the maximum number of Pb (II) ions to be adsorbed at the optimal parameters pH of 5.5 for LHMDIC and pH of 8 for LPDIC, the concentration of 50 ppm, and dose of 50 mg at 25^{o}C. The results are shown in figure 3.13 in appendix b over a period of 5-60 minutes.

According to figure 3.13, the first five minutes saw the best adsorption of both polymers. This is because the active sites are sufficiently exposed, and the adsorbent has a big surface area. After 5 minutes, the adsorption of Pb(II) ions for both polymers were decreased, because there are no longer any vacancies for the Pb(II) ions to bind to, after that the adsorption process has become practically constant throughout the course of 10 to 60 minutes [123]

3.4.5 Effect of Temperature

In order to determine the optimum temperature at which the greatest quantity of lead ions may be eliminated by using both LHMDIC and LPDIC, the experiments were conducted at the optimal parameters of pH 5.5 for LHMDIC and pH of 8 for LPDIC, the concentration of 50 ppm, and dose of 50 mg at 25ºC. The results are shown in figure 3.14 in appendix b for various temperatures (5, 10, 20, 40, and 50 ºC).

According to the findings, it is noted that the removal of Pb(II) ions increased slightly at first 10 minutes due to the dissociation of protons from surface functional groups for LHMDIC and LPDIC polymers, which produces more adsorption sites. The Pb(II) ions also gain kinetic energy as a result of the temperature rise, which promotes diffusion and speeds up the adsorption process [124]. For LPDIC polymer, there are decrease in the uptake of Pb(II) ions by increasing temperature to 20ºC.

3.5 Ideal adsorption conditions

3.6 Adsorption Isotherm

A heavy metal's affinity for binding species can be measured using adsorption isotherms. To construct an isotherm, several dosages of the adsorbent are applied to a known quantity of adsorbate in a fixed volume of liquid.

3.6.1 Langmuir Isotherm

The Langmuir (ppm).

K_l: The adsorption energy-related Langmuir affinity constant (L/mg)

The results in table 3.4 in appendix a show that both polymers have $R_L < 1$, which denotes that the adsorption is favorable. For LPDIC polymer that has R^2 near to 1, is consider more favorable and follows the Langmuir model more than HMDIC.

3.6.2 Freundlich Isotherm

Compared to the Langmuir isotherm, Freundlich isotherm is often better at describing adsorption in a water medium. The multilayer adsorption and adsorption processes on heterogeneous surfaces are discussed and described using the Freundlich isotherm model. The nonlinear equation 6 often provides this isotherm.

$$\ln q_e = \ln K_f + 1/n \ln C_e \qquad \text{Eq .6}$$

The Freundlich constant (K_f), which is correlated with the adsorption capacity (mg/g), is a physical constant.

The letter n is used to indicate the heterogeneity coefficient (g/L).

Adsorption will follow this model if the graph of lnq vs lnc shows a straight line with an R^2 value near 1.

As can be seen in table 3.7 in appendix b, both the LHMDIC and LPDIC polymer have R^2 values with the Freundlich isotherm that are extremely close to 1. obeys this concept, with the adsorption process occurring not only at the polymer's surface but also in its multilayers.

3.7 Kinetic Adsorption

Adsorption must be investigated kinetically by tracking the rate of adsorption and determining whether it is impacted by the predetermined conditions in order to comprehend the adsorption process mechanism. To examine adsorbent effectiveness and adsorption mass transfer mechanisms, adsorption kinetic models were used. Studying the outcomes using kinetic principles, like pseudo-first order and pseudo-second order, is necessary to describe the mechanism by which metal ions are adsorbed.

3.7.1 Pseudo-first-order model

The pseudo-first-order equation's linear form is given as:

$$\ln (q_e - q_t) = \ln q_e - K_1 t \qquad \text{Eq .7}$$

K_1: the first-order rate constant (min^{-1})

q_e: the equilibrium solute absorption rate expressed in (mg/g) of adsorbent.

q_t: the solute absorption rate per unit weight of the adsorbent at any particular time (mg/g).

If the ln (q_e- q_t) vs. time graph displays a straight line with a high R^2 value, the adsorption complies with this model.

3.7.2 Pseudo-second-order model

The pseudo-second-order equation's linear form is given as:

$$t/q_t = 1/k_2 q^2_e + t/q_e \qquad \text{Eq .8}$$

K_2: is the second-order rate constant (g mg-1 min-1)

q_e: is the equilibrium solute absorption rate per unit weight of adsorbent (mg/g).

At any given time, the quantity of solute adsorbed is measured as a function of adsorbent weight, or q_t (mg/g)

The adsorption will follow this model if the plot of t/q_t vs. time shows a straight line with an approximate R^2 value.

It was determined which order the reaction will follow by the correlation coefficient's (R^2) value. According to correlation coefficients (R^2) of pseudo-first and second order, the Pb(II) ion adsorption on LHMDIC polymers appears to follow pseudo-second order since (R^2 = 0.9999) in this case is higher than (R^2 = 0.3193) obtained by applying pseudo-first-order. Also LPDIC polymers appears to follow pseudo-second order since (R^2 = 1). Additionally, both polymers exhibit greater q_e theo. and q_e exp. values in the pseudo-second order compared to the pseudo-first order.

3.8 Thermodynamic Experiments

Studies on thermodynamics were conducted at various temperatures for the aim of investigating thermodynamics, and the estimated parameters were enthalpy (H), entropy (S), and Gibbs free energy change (G). Important design elements include measurable thermodynamic

characteristics such as temperature. The process' spontaneity and viability are determined by these factors and by using the thermodynamic equation of the Van't Hoff plot ($\Delta G = \Delta H - T\Delta S$). The thermodynamic parameters (H° and S°) of lead ion absorption on both samples of LHMDIC and LPDIC can be calculated using the slope and y-intercept of the graph ln (K_d) against (1/T).

Table 3.17 in appendix a demonstrates that the adsorption of Pb(II) ion on LPDIC polymers is spontaneous because all $\Delta \mathbf{G°}$ values are negative; a spontaneous process is one that takes place without the addition of external energy; in contrast, the adsorption of Pb(II) ion on LHMDIC polymer is nonspontaneous as shown in table 3.16 in appendix a. The fact that both polymers have negative $\Delta H°$ indicates that the process is exothermic in nature. The declining randomness between metal ions is indicated by the negative $\Delta \mathbf{S°}$ for both polymers.

3.9 Purification of Wastewater

The effectiveness of the sulfated ester with LHMDIC and LPDIC toward the removal of heavy metal ions were both assessed using an actual sample of wastewater, as was previously described (sec. 2.8).

Table 3.19 in appendix a demonstrates a high efficiency for the removal of hazardous metal ions, including Cd, Pb, Cu, Zn, and Al, at high concentrations of 50 mg of LHMDIC polymer, with removal efficiencies of 96%, 91%, 89%, 89%, and 82% respectively. For polymer LPDIC was employed to remove a number of heavy metals at a concentration of 50 mg. According to the findings, Cd, Pb, Cu, Zn, and Al had efficient removal rates of 92%, 89%, 88%, 82%, and 80%, respectively.

3.10 Conclusions

According to the results of the experiments, LHMDIC and LPDIC are both effective adsorbents for removing Pb(II) ions from synthetic OILW wastewater. The thermal curing of the polymers shows how the mass of LHMDIC reduces as the temperature increases up to 400 °C before stabilizing at 700 °C. The mass of LPDIC is initially steady, and then starts to drop as the temperature increases from 250 °C to 600 °C. We find commonalities between the two polymers at 700 °C, which causes an amazing 90% mass loss. IR and TGA were used to characterize the polymer after curing. Temperature, pH, dose, concentration, contact time, and dosage to investigate the optimum adsorption condition, variables were explored. The optimal value of the investigated parameters for LHMDIC was around 5.5 pH, 50.00 mg dosage, 50.00 ppm concentration, 5.00 min of contact time, and 10°C. The conditions for LPDIC were pH 8, 50.0 mg dosage, 50.00 ppm concentration, 5.00 min contact duration, and 10°C.

The maximum removal efficiency was determined to be 99.95% for LHMDIC and 98.75% for LPDIC. This application for Pb(II) ion removal efficiency for a genuine sewage sample showed outstanding removal. The Pb(II) ion appears to follow pseudo-second order in the Pb(II) ion adsorption on LHMDIC and LPDIC polymers because (R^2 = 0.9999) and (R^2 = 1), respectively, of the reaction's isotherm, kinetics, and thermodynamic studies. LHMDIC exhibit favorable adsorption and follow the Langmuir mode according to the reaction isotherm, which has R< 1. Both the R^2 values with the Freundlich isotherm for the LHMDIC and LPDIC polymer are very near to 1, which obeys this idea, with the adsorption process taking place both at the polymer's surface and within its multilayers. All values of G° are negative, indicating that the Pb(II) ion adsorption on LPDIC polymers is spontaneous. In contrast, the Pb(II) ion adsorption on LHMDIC polymer is nonspontaneous. The process is exothermic because both polymers have negative H°. The negative S° and the negative biomass for both polymers both signify a decreasing randomness between metal molecules.

3.11 Recommendations

- Increasing active sites in order to increase the removal efficacy by adding more drops of triethylamine
- Increasing the polymer's surface area by applying nanoscale technology.
- The polymers can be enhanced by adding additional components to improve its absorption efficiency.
- The surface area of the polymer can be increased by using Nano-scale technique.
- Development can also be accomplished by preparing alternative ratios and testing their efficiency in preventing harmful chemical absorption.
- Polymers applicability can be used in other sectors, including medicine and purification of materials used in industry.

List of Abbreviations

Abbreviations	Meaning
OISW	Olive Industry Solid Waste
OILW	Olive Industry Liquid Waste
WHO	World Health Organization
LiP	Lignin peroxidases
MnP	Manganese peroxidases
BOD	Blood Oxygen Demand
OIW	Olive IndustryWaste
OMW	Olive Mill Waste
OMSW	Olive Mill Solid Waste
MB	Methelene Blue
TIPS	Thermally Induced Phase Separation
HCFCs	Hydrochlorofluorocarbons
TGA	thermo gravimetric analyzer
DSC	differential scanning calorimetry
ICP-MS	Inductively Coupled Plasma Mass Spectrometry
FAAS	Flame Atomic Absorption Spectrometer
AFM	Atomic Force Microscope
LHMDIC	1,4-hexamethylene diisocyanate
LPDIC	1,4-phenylne diisocyanate
λ	TheWavelength (nm)
R^2	The Correlation coefficient (regression coefficient, fitting coefficient)
ΔG°	The modification of Gibbs free energy (J).
ΔH°	The enthalpy change (J)
ΔS°	The entropy change (J/K)
T	The stands for the actual temperature (K).
K	The thermodynamic equilibrium constant (L/g)
K_d	The constant of thermodynamic equilibrium
R	The universal gas constant, equaling 8.314 J.mol-1
M	The adsorbent's mass (g)

C_i	The stands for the solution's initial concentration of heavy metal ions (ppm)
C_f	The final heavy metal ion concentrations in solution (ppm)
Q_{max}	The maximum monolayer adsorption capacity of the adsorbent (in mg/g)
q_e	The mass of adsorbate adsorbed per unit mass of the polymer (mg/g)
C_e	The ion equilibrium concentration (ppm)
K_1	The first-order rate constant (min^{-l})
K_2	The second-order rate constant (g mg-1 min-1)
K_f	Freundlich constant
q_t	Amount of adsorbate per unit mass of adsorbent at time t (min)

References

[1] Elehinafe, F. B., Agboola, O., Vershima, A. D., & Bamigboye, G. O. (2022). Insights on the Advanced Separation Processes in Water Pollution Analyses and Wastewater Treatment–A Review. *South African Journal of Chemical Engineering.*

[2] Schwarzenbach, R. P., Egli, T., Hofstetter, T. B., Von Gunten, U., & Wehrli, B. (2010). Global water pollution and human health. *Annual review of environment and resources,* 35(1), 109-136.

[3] Kumar, V., Othman, N., & Asharuddin, S. (2018). Applications of natural coagulants to treat wastewater− a review. *In MATEC Web of Conferences* (Vol. 103, p. 06016). EDP Sciences.

[4] Chaudhry, F. N., & Malik, M. F. (2017). Factors affecting water pollution: a review. *J Ecosyst Ecography*, 7(225), 1-3.

[5] Lakherwal, Dimple. (2014). "Adsorption of heavy metals: a review." *International journal of environmental research and development*. 4.1: 41-48.

[6] Tripathi, Ashutosh, and M. Rawat Ranjan. (2015). "Heavy metal removal from wastewater using low cost adsorbents." *J Bioremed Biodeg* 6.6: 315

[7] Sharma, Pushpendra Kumar, Sohail Ayub, and Chandra Nath Tripathi. (2013). "Agro and horticultural wastes as low cost adsorbents for removal of heavy metals from wastewater: A review." *International Refereed Journal of Engineering and Science* 2.8:18-27.

[8] Renu Bisht. Madhu Agarwal.Kailash Singh.(2017). Methodologies for removal of heavy metal ions from wastewater: an overview. 2017.*Interdisciplinary Environmental Review18*(2):124-142. DOI:10.1504/IER.2017.10008828

[9] Acharya, Jyotikusum, Upendra Kumar, and P. Mahammed Rafi.(2018). "Removal of heavy metal ions from wastewater by chemically modified agricultural waste material as potential adsorbent-a review." *International Journal of Current Engineering and Technology* 8.3: 526-530.

[10] Chakraborty, R., Asthana, A., Singh, A. K., Jain, B., & Susan, A. B. H. (2022). Adsorption of heavy metal ions by various low-cost adsorbents: a review. *International Journal of Environmental Analytical Chemistry*, 102(2), 342-379.

[11] Salam, Omar E. Abdel, Neama A. Reiad, and Maha M. ElShafei. (2011)."A study of the removal characteristics of heavy metals from wastewater by low-cost adsorbents." *Journal of Advanced Research* 2.4: 297-303

[12] Srivastava, N. K., & Majumder, C. B. (2008). Novel biofiltration methods for the treatment of heavy metals from industrial wastewater. *Journal of hazardous materials*, 151(1), 1-8.

[13] de Souza, C. B., & Silva, G. R. (2019). Phytoremediation of effluents contaminated with heavy metals by floating aquatic macrophytes species. *IntechOpen.*

[14] Singh, R., Gautam, N., Mishra, A., & Gupta, R. (2011). Heavy metals and living systems: An overview. *Indian journal of pharmacology*, *43*(3), 246.

[15] Weiss, B. and P.J.J.E.h.p. Landrigan. (2000). The developing brain and the environment: *an introduction*. 108(suppl 3): p. 373-374.

[16] Mousavi, H. Z., Hosseynifar, A., Jahed, V., & Dehghani, S. A. M. (2010). Removal of lead from aqueous solution using waste tire rubber ash as an adsorbent. *Brazilian Journal of Chemical Engineering*, *27*, 79-87.

[17] Tchounwou, P. B., Yedjou, C. G., Patlolla, A. K., & Sutton, D. J. (2012). Heavy metal toxicity and the environment. *Molecular, clinical and environmental toxicology*, 133-164.

[18] Huda, Bonusa Nabila, Endang Tri Wahyuni, and Mudasir Mudasir. (2021). "Eco-friendly immobilization of dithizone on coal bottom ash for the adsorption of lead (II) ion from water." *Results in Engineering* 10: 100221.

[19] Raikar, Rajkumar V., Sefra Correa, and Praveen Ghorpade. (2015). "Removal of lead (II) from aqueous solution using natural and activated rice husk." *International Research Journal of Engineering and Technology* 2.03: 1677-1685.

[20] Guo, X., Zhang, S., & Shan, X. Q. (2008). Adsorption of metal ions on lignin. *Journal of hazardous materials,* 151(1), 134-142.

[21] Ahalya, N., Ramachandra, T. V., & Kanamadi, R. D. (2003). Biosorption of heavy metals. *Res. J. Chem. Environ*, *7*(4), 71-79.

[22] Shrestha, R., Ban, S., Devkota, S., Sharma, S., Joshi, R., Tiwari, A. P., ... & Joshi, M. K. (2021). Technological trends in heavy metals removal from industrial wastewater: A review. *Journal of Environmental Chemical Engineering*, 9(4), 105688.

[23] Medeiros, A. D. L. M. D., Silva Junior, C. J. G. D., Amorim, J. D. P. D., Durval, I. J. B., Costa, A. F. D. S., & Sarubbo, L. A. (2022). Oily Wastewater treatment: Methods, challenges, and trends. *Processes*, *10*(4), 743.

[24] Kanamarlapudi, S. L. R. K. , Kumar Chintalpudi, V., & Muddada, S. (2018). Application of Biosorption for Removal of Heavy Metals from Wastewater. In J. Derco, & B. Vrana (Eds.), *Biosorption*. *IntechOpen*.

https://doi.org/10.5772/intechopen.77315.

[25] Kratochvil, D., & Volesky, B. (1998). Advances in the biosorption of heavy metals. *Trends in biotechnology*, 16(7), 291-300.

[26] Abbas, S. H., Ismail, I. M., Mostafa, T. M., & Sulaymon, A. H. (2014). Biosorption of heavy metals: a review. *J Chem Sci Technol*, 3(4), 74-102.

[27] Somorjai, G.A. and Y. Li, (2010). Introduction to surface chemistry and catalysis.: John Wiley & Sons.

[28] Kulkarni Vishakha, S., Butte Kishor, D., & Rathod Sudha, S. (2012). Natural polymers– A comprehensive review. *International journal of research in pharmaceutical and biomedical sciences*, 3(4), 1597-1613.

[29] Awaleh, M. O., & Soubaneh, Y. D. (2014). Waste water treatment in chemical industries: the concept and current technologies. *Hydrology: Current Research*, 5(1), 1.

[30] Dongre, R. S., Sadasivuni, K. K., Deshmukh, K., Mehta, A., Basu, S., Meshram, J. S.& Karim, A. (2019). Natural polymer based composite membranes for water purification: a review. *Polymer-Plastics Technology and Materials*, 58(12), 1295-1310.

[31] Theodoro, J. P., Lenz, G. F., Zara, R. F., & Bergamasco, R. (2013). Coagulants and natural polymers: perspectives for the treatment of water. *Plastic and Polymer Technology*, 2(3), 55-62.

[32] Kumar, A., Chandra, R. (2020). Ligninolytic enzymes and their mechanisms for degradation of lignocellulosic waste in the environment. www.cell.com/heliyon. Heliyon 6, e03170.

[33] Hamouda, R. A., & Abdel-Hamid, M. S. (2022). A Comparative Study of Cellulose Nanocomposite Derived from Algae and Bacteria and Its Applications. In Advances in Nanocomposite Materials for Environmental and Energy Harvesting Applications (pp. 151-187). Springer, *Cham*.

[34] O'Connell, D. W., Birkinshaw, C., & O'Dwyer, T. F. (2008). Heavy metal adsorbents prepared from the modification of cellulose: A review. *Bioresource Technology*, 99(15), 6709–6724.

https://doi.org/10.1016/J.BIORTECH.2008.01.036.

[35] Ahmad, M., Ahmed, S., Swami, B. L., & Ikram, S. (2015). Adsorption of heavy metal ions: role of chitosan and cellulose for water treatment. *Langmuir,* 79, 109-155.

[36] Lee, J.; Patel, R. (2022). Wastewater Treatment by Polymeric Microspheres: A Review.. *Polymers*, 14, 1890. https://doi.org/ 10.3390/polym14091890.

[37] Kamel, S., Hassan, E.M., El-Sakhawy, M., (2006). Preparation and application of acrylonitrile-grafted cyanoethyl cellulose for the removal of copper(II) ions. *Journal of Applied Polymer Science* u, P., Gachanja, A., Mugo, S., Murigi, M., Kairigo, P. K., & Njonge, F. 100, 329–334.

[38] Madivoli, E., Karer Adsorption of selected heavy metals on modified nano cellulose.

[39] El-Khouly, A. S., Takahashi, Y., Saafan, A. A., Kenawy, E., & Hafiz, Y. A. (2011). Study of heavy metal ion absorbance by amidoxime group introduced to cellulose-graft- polyacrylonitrile. *Journal of Applied Polymer Science*, 120(2), 866-873.

[40] Sun, X., Peng, B., Ji, Y., Chen, J., & Li, D. (2009). Chitosan (chitin)/cellulose composite biosorbents prepared using ionic liquid for heavy metal ions adsorption. *AIChE journal*, 55(8), 2062-2069.

[41] Gurgel, L. V. A., Júnior, O. K., de Freitas Gil, R. P., & Gil, L. F. (2008). Adsorption of Cu (II), Cd (II), and Pb (II) from aqueous single metal solutions by cellulose and mercerized cellulose chemically modified with succinic anhydride. *Bioresource technology*, 99(8), 3077-3083.F.

[42] Asadi, F., Shariatmadari, H., & Mirghaffari, N. (2008). Modification of rice hull and sawdust sorptive characteristics for remove heavy metals from synthetic solutions and wastewater. *Journal of hazardous materials*, 154(1-3), 451-458.

[43] Niinimaa J and Sillanpää M. (2014). Adsorption of Ni(II), Cu(II) and Cd(II) from aqueous solutions by amino modified nanostructured microfibrillated cellulose. *Cellulose*; 21(3): 1471-1487.

[44] Kardam, A., ROHIT, R. K., & Srivastava, S. (2012). Hu, L., Du, M., & Zhang, J. (2017). Hemicellulose-based hydrogels present status and application prospects: A brief review. *Open Journal* of Forestry, 8(1), 15-28.

[45] Luo, Y., Li, Z., Li, X., Liu, X., Fan, J., Clark, J. H., & Hu, C. (2019). The production of furfural directly from hemicellulose in lignocellulosic biomass: A review. *Catalysis Today*, 319, 14-24.

[46] Huang, L. Z., Ma, M. G., Ji, X. X., Choi, S. E., & Si, C. (2021). Recent Developments and Applications of Hemicellulose from wheat straw: A review. *Frontiers in Bioengineering and Biotechnology*, 9, 440.

[47] Lu, Y., He, Q., Fan, G., Cheng, Q. & Song, G. (2021). Extraction and modification of hemicellulose from lignocellulosic biomass: A review. *Green Processing and Synthesis*, 10(1), 779-804. https://doi.org/10.1515/gps-2021-0065.

[48] Ban, W., Chen, X., Andrews, G., & Van Heiningen, A. (2011). Influence of hemicelluloses pre-extraction and re-adsorption on pulp physical strength. II. Beatability and strength study. *Cellulose Chemistry and Technology*, 45(9), 633.

[49] Cheng, H. L., Feng, Q. H., Liao, C. A., Liu, Y., Wu, D. B., & Wang, Q. G. (2016). Removal of methylene blue with hemicellulose/clay hybrid hydrogels. *Chinese Journal of Polymer Science*, 34(6), 709-719.

[50] Ayoub, A., Venditti, R. A., Pawlak, J. J., Salam, A., & Hubbe, M. A. (2013). Novel hemicellulose–chitosan biosorbent for water desalination and heavy metal removal. *ACS Sustainable Chemistry & Engineering*, 1(9), 1102-1109.

[51] Mohammadabadi, S. I., & Javanbakht, V. (2020). Ultrasonic assisted hydrolysis of barley straw biowastes into construction of a novel hemicellulose-based adsorbent and its adsorption properties for Pb2+ ions from aqueous solutions. *Renewable Energy*, 161, 893-906.

[52] Peng, X. W., Zhong, L. X., Ren, J. L., & Sun, R. C. (2012). Highly effective adsorption of heavy metal ions from aqueous solutions by macroporous xylan-rich hemicelluloses-based hydrogel. *Journal of agricultural and food chemistry*, 60(15), 3909-3916.

[53] Ferrari, E., Ranucci, E., Edlund, U., & Albertsson, A.-C. (2014). Design of Renewable Poly(Amidoamine)/Hemicellulose Hydrogels for Heavy Metal Adsorption. *Journal of Applied Polymer Science*, 132, 41695 p. https://doi.org/10.1002/app.41695.

[54] Naseer, A., Jamshaid, A., Hamid, A., Nawshad, M., Ghauri, M.,Iqbal, J., Rafiq, S., Khuram, Sh., Shah, N. S.(2019). Lignin and Lignin Based Materials for the Removal of Heavy Metals from Waste Water-An Overview. Z. *Phys. Chem.*; 233(3): 315–345.

[55] Li, Z.; Ge, Y.; Wan, L. (2015). Fabrication of a green porous ligninbased sphere for the removal of lead ions from aqueous media. *J. Hazard. Mater.*, 285 (0), 77.

[56] Yao, Q., Xie, J., Liu, J., Kang, H., & Liu, Y. (2014). Adsorption of lead ions using a modified lignin hydrogel. *Journal of Polymer Research*, 21(6), 1-16.

[57] Lalvani, S. B., Wiltowski, T. S., Murphy,D., Lalvani,L. S. (1997). Metal removal from process water by lignin. *Environmental Technology*, Vol. 18. Pp 1163-1168.

[58] Boerjan, W., Ralph, J., Baucher, M. (2003). Lignin Biosynthesis. *Annu. Rev. Plant Biol.*, 54519–546, https://doi.org/https://doi.org/10.1146/annurev.arplant.54.031902.

[59] Vanholme, R., Demedts, B., Morrell, K., Ralph, J., Boerjan, W. (2010). Lignin Biosynthesis and Structure, *Plant Physiol.* 153,895–905 https://doi.org/10.1104/pp.110.155119.

[60] Rinaldi, R., Jastrzebski, R., Clough, M.T., Ralph, J., Kennema, M., Bruijnincx, P.C.A., Weckhuysen, B.M. (2016). Paving the way for lignin valorization: recent advances in bioengineering, biorefining, and catalysis. *Angew. Chem. Int. Ed.* 55, 8164– 8215.https://doi.org/10.1002/anie.201510351.

[61] Ragauskas, A.J., Beckham, G.T., Biddy, M.J., Chandra, R., Chen, F., Davis, M.F., Davison, B.H., Dixon, R.A., Gilna, P., Keller, M. Langan, P. Naskar, A.K., Saddler, J.N. Tschaplinski, T.J., Tuskan, G.A., Wyman, C.E. (2014). Lignin valorization: improving lignin processing in the biorefinery. *Science* 344, 1246843https://doi.org/10. 1126/science.1246843.

[62] Francisco, J., Dueñas, J. ,Martínez, Á. T. (2009). Microbial degradation of lignin: how a bulky recalcitrant polymer is efficiently recycled in nature and how we can take advantage of this. Centro de Investigaciones Biológicas, CSIC, Ramiro deMaeztu 9, E-28040 Madrid, Spain. *Microbial Biotechnology*. 2(2), 164–177.

[63] German C. Quintana, G. J. M. Rocha, A. R. Goncalves, J. A. Velasquez. (2008). Evaluation of heavy metal removal by oxidized lignins in acid media from various sources. *JOURNAL HOME PAGE*. Home > Vol 3, No 4 > Quintana.

[64] Ralph, J., Akiyama, T., Kim, H., Lu, F., Schatz, P.F., Marita, J.M., Ralph, S.A., Reddy, M.S., Chen, F., Dixon, R.A. (2006). Effects of coumarate 3- hydroxylase down-regulation on lignin structure. *J Biol Chem*, 281:8843-8853.

[65] Sarkanen, K.V., Ludwig, C.H. (1971). Lignins. *John Wiley&Sons*, Inc., New York, p.226.T.

[66] Bonawitz, N.D., Chapple, C. (2010).The genetics of lignin biosynthesis: connecting genotype to phenotype. *Annu Rev Genet*, 44:337-363.

[67] Beis, TS.H., Mukkamala, S., Hill, N., Joseph, J., Baker, C., Jensen, B., Stemmler,M.C. Wheeler, E.A., Frederick, B.G., Heiningen, A.v., Berg, A.G., DeSisto, W.J. (2010). Fast pyrolysis of lignins. *BioResources* 5. 1408–1424.

[68] Brebu, M., Cazacu, G., Chirila, O. (2011). Pyrolysis of lignin – a potential method for obtaining chemicals and/or fuels, Cell. *Chem. Technol*. 45, 43–50.

[69] Choi, H. S., Meier, D., & Windt, M. (2012). Rapid screening of catalytic pyrolysis reactions of Organosolv lignins with the vTI-mini fast pyrolyzer. *Environmental Progress & Sustainable Energy*, 31(2), 240-244.

[70] Rahman, Md.M., Liu, R., Cai, J. (2018). Catalytic fast pyrolysis of biomass over zeolites for high-quality bio-oil - a review, Fuel Process. *Technol.* 180, 32–46, https://doi.org/10.1016/j.fuproc.2018.08.002.

[71] Villar, J.C., Capers, A., García-Ochoa, F. (2001). Oxidation of hardwood kraft-lignin to phenolic derivatives with oxygen as oxidant. *Wood Sci. Technol*. 35, 245–255, https://doi.org/10.1007/s002260100089.

[72] Mathias, A.L., Rodrigues, A.E. (1995). Production of Vanillin by Oxidation of Pine KraftLignins with Oxygen. *Holzforschung*. 49, 273–278, https://doi.org/10.1515/hfsg.1995.49.3.273.

[73] Khindaria, A., Yamazaki, I., Aust, S.D. (1995). Veratryl alcohol oxidation by lignin peroxidase. *Biochemistry*, 34:16860-16869. 16.

[74] Hofrichter, M.(2002). Lignin conversion by manganese peroxidase. *Enzyme Microb Technol*, 30:454-466. 20.

[75] Choinowski, T., Blodig, W., Winterhalter, K. H., & Piontek, K. (1999). The crystal structure of lignin peroxidase at 1.70 Å resolution reveals a hydroxy group on the Cβ of tryptophan 171: a novel radical site formed during the redox cycle. *Journal of molecular biology*, 286(3), 809-827.

[76] Tien, M., Kirk, T.K. (1984). Lignin-degrading enzyme from Phanerochaetechrysosporium: purification, characterization, and catalytic properties of a unique H2O2-requiring oxygenase. Proc Natl Acad Sci U S A, 81:2280-2284.

[77] Glenn, J.K., Gold, M.H.(1985). Purification and characterization of an extracellular Mn(II)-dependent peroxidase from the lignin-degrading basidiomycete, Phanerochaetechrysosporium. *Arch BiochemBiophys*, 242:329-341.

[78] Kuan, I.C., Johnson, K.A., Tien, M.(1993). Kinetic analysis of manganese peroxidase. The reaction with manganese complexes. *J Biol Chem*, 268:20064-20070.

[79] Camarero, S., Sarkar, S., Ruiz-Duen˜ as F.J., Martı´nez, M.J., Martı´nez,A´.T.(1999). Description of a versatile peroxidase involved in the

natural degradation of lignin that has both manganese peroxidase and lignin peroxidase substrate interaction sites. *J Biol Chem*, 274:10324-10330.

[80] Wong, W.S.D. (2009). Structure and action mechanism of ligninolytic enzymes. Appl. Biochem. *Biotechnol*. 157, 174–209.

[81] Todorciuc, T.; Bulgariu, L.; Popa, V. I. (2015). Adsorption of Cu(II) from aqueous solution on wheat straw lignin: Equilibrium and kinetic studies. *Cell Chem*. Technol. 49 (5−6), 439−447.

[82] Albadarin, A. B.; Al-Muhtaseb, A. a. H.; Walker, G. M.; Allen, S. J.; Ahmad, M. N. M. (2011). Retention of toxic chromium from aqueous phase by H3PO4-activated lignin: Effect of salts and desorption studies? *Desalination*, 274, 64

[83] Merdy, P.; Guillon, E.; Aplincourt, M.; Dumonceau, J.; Vezin, H. (2002). Copper sorption on a straw lignin: Experiments and EPR characterization. J. *Colloid Interface Sci*. 245 (1), 24.

[84] Acemiolu, B.; Samil, A.; Alma, M. H.; Gundogan, R. (2003). Copper(II) removal from aqueous solution by organosolv lignin and its recovery. J. Appl. *Polym*. Sci. 89 (6), 1537.

[85] Demirbas, A. (2004). Adsorption of lead and cadmium ions in aqueous solutions onto modified lignin from alkali glycerol delignication. J. *Hazard. Mater*., 109 (1−3), 221.

[86] Wei, Yi, Jijian Hong, and Weirong Ji. (2018). "Thermal characterization and pyrolysis of digestate for phenol production." *Fuel* 232: 141-146.

[87] Yang, Haiping, et al. (2021). "Lignin pyrolysis under NH3 atmosphere for 4-vinylphenol product: An experimental and theoretical study." *Fuel* 297: 120776.

[88] Qin, L.; Ge, Y.; Deng, B.; Li, Z. (2017). Poly (ethylene imine) anchored lignin composite for heavy metals capturing in water. J. Taiwan Inst. Chem. Eng., 71, 84.

[89] Kong, Wen, et al.(2016). "Characterization of a novel manganese peroxidase from white-rot fungus Echinodontium taxodii 2538, and its use for the degradation of lignin-related compounds." *Process Biochemistry* 51.11: 1776-1783.

[90] Shi, Lili, et al. (2014). "Biochemical and molecular characterization of a novel laccase from selective lignin-degrading white-rot fungus Echinodontium taxodii 2538." *Process Biochemistry* 49.7 : 1097-1106.+

[91] Khdair, A., & Abu-Rumman, G. (2020). Sustainable environmental management and valorization options for olive mill byproducts in the Middle East and North Africa *(MENA) region. Processes*, 8(6), 671.

[92] Azbar, N., Bayram, A., Filibeli, A., Muezzinoglu, A., Sengul, F., and Ozer, A. (2004). "A review of waste management options in olive oil production" Crit. Rev. *Environ. Sci. Technol*.,34, 209-247.

[93] Shaheen, H., & Karim, R. A. (2007). Management of olive-mills wastewater in Palestine.

[94] Ayrilmis, N., and Buyuksari, U. (2010). "Utilization of olive mill sludge in the manufacture of fiberboard".*BioResources*, 5, 1859-1867.

[95] Azbar, N., Ursillo, P., & Speece, R. E. (2001). Effect of process configuration and substrate complexity on the performance of anaerobic processes. *Water research*,

[96] Ghannam, M., Al-Sa'ed, R., & Zimmo, O. (2005). Assessment of recycling perspectives for olive mill solid waste in Palestine

[97] Bhatnagar, A., Kaczala, F., Hogland, W., Marques, M., Paraskeva, C. A., Papadakis, V. G., & Sillanpää, M. (2014). Valorization of solid waste products from olive oil industry as potential adsorbents for water pollution control—a review. *Environmental Science and Pollution Research*, 21(1), 268-298.

[98] Ouazzane, H., et al. (2017). Olive mill solid waste characterization and recycling opportunities: *A review*. 8(8): p. 2632-2650.

[99] Chouchene, A., Jeguirim, M., Khiari, B., Zagrouba, F., & Trouvé, G. (2010). Thermal degradation of olive solid waste: Influence of particle size and oxygen concentration. *Resources, Conservation and Recycling*, 54(5), 271-277.

[100] Flouri, F., Sotirchos, D., Ioannidou, S., & Balis, C. (1996). Decolorization of olive oil mill liquid wastes by chemical and biological means. *International Biodeterioration & Biodegradation*, 38(3-4), 189-192.

[101] Pierantozzi, P., Zampini, C., Torres, M., Isla, M. I., Verdenelli, R. A., Meriles, J. M., & Maestri, D. (2012). Physico-chemical and toxicological assessment of liquid wastes from olive processing-related industries. *Journal of the Science of Food and Agriculture*, 92(2), 216-223.

[102] Muscolo, A., Sidari, M., Mallamaci, C., & Attinà, E. (2010). Effects of olive mill wastewater on seed germination and seedling growth. *Terrestrial and Aquatic Environmental Toxicology*, 4(1), 75-83.

[103] Tsagaraki, E., Lazarides, H. N., & Petrotos, K. B. (2007). Olive mill wastewater treatment in utilization of by-products and treatment of waste in the food industry (pp. 133-157). *Springer, Boston*, MA.

[104] Celik, A., Demirbas, A., (2005). Removal of heavy metal ions from aqueous solutionsvia adsorption onto modified lignin from pulping wastes. *Energy*. Sources 27,1167-1177.

[105] Conrad, K., (2008). Correlation between the distribution of lignin and pectin and distribution of sorbed metal ions (lead and zinc) on coir. (Cocos nucifera L.). *Bioresour. Technol*. 99, 8476-8484.

[106] Wu, Y.; Zhang, S. Z.; Guo, X. Y.; Huang, H. L. (2008). Adsorption of chromium(III) on lignin. *Bioresour. Technol*. 2008, 99 (16), 7709. (45) .

[107] Liu, X.L., Zhu, H.X., Qin, C.R., Zhou, J.H., Zhao, J.R., Wang, S.F., (2013). Adsorption of heavy metal ion from aqueous single metal solution by aminated epoxy-lignin. *Bioresources*. 8, 2257-2269.

[108] Hemmilä, V., Trischler, J., Sandberg, D.(2013). Wood Sci. Eng. *Proc*. 9th Meet. 98.

[109] Janusz, G., Pawlik, A., Sulej, J., Burek, U.S., Wilkołazka, A.J., Paszczynski, A.(2017). Lignin degradation: microorganisms, enzymes involved, genomes analysis and Evolution. *FEMS Microbiology Reviews fux*049 41, 941–962.

[110] Yao, Q., Xie, J., Liu, J., Kang, H., & Liu, Y. (2014). Adsorption of lead ions using a modified lignin hydrogel. *Journal of Polymer Research*, 21(6), 1-16.

[111] MuhammadUsman[ab]AdeelAhmed[a]BingYu[ab]SongWang[a]YouqingShen[a]HailinCon g.(2021).Simultaneous adsorption of heavy metals and organic dyes by β-

Cyclodextrin-Chitosan based cross-linked adsorbent. *Carbohydrate Polymers* Volume 255, 1 March 2021, 117486

[112] Usman, M., Ahmed, A., Yu, B., Wang, S., Shen, Y., & Cong, H. (2021). Simultaneous adsorption of heavy metals and organic dyes by β-Cyclodextrin-Chitosan based cross-linked adsorbent. *Carbohydrate polymers*, *255*, 117486.

[113] Utzeri, G.; Verissimo, L.; Murtinho, D.; Pais, A.A.C.C.; Perrin, F.X.; Ziarelli, F.; Iordache, T.-V.; Sarbu, A.; Valente, A.J.M. (2021). Poly(β-cyclodextrin)-Activated Carbon Gel Composites for Removal of Pesticides from Water. *Molecules*, 26, 1426. https://doi.org/10.3390/molecules26051426.

[114] Duan,D.Lei,H.Wang,Y.Ruan,R. Liu,Y. Ding,L. Zhang,Y. Liu,L. (2019). Renewable phenol production from lignin with acid pretreatment and ex-situ catalytic pyrolysis. *Journal of Cleaner Production.* Volume 231, Pages 331-340.

[115] Zeng ،J. ،Yoo ،CG ،Wang ،F. ،Pan ،X. ،Vermerris ،W. and Tong ،Z.(2015). *ChemSusChem*. 8: 861-871. https://doi.org/10.1002/cssc.201403128

[116] Yan, Jiang, et al. (2020). "Selective valorization of lignin to phenol by direct transformation of Csp2–Csp3 and C–O bonds." *Science advances* 6.45: eabd1951.

[117] Wang, Chenxi, et al. (2021). "Integrated harvest of phenolic monomers and hydrogen through catalytic pyrolysis of biomass over nanocellulose derived biochar catalyst." *Bioresource Technology*. 320: 124352.

[118] Lee, S. T. (2004). Introduction: polymeric foams, mechanisms, and materials. *In Polymeric foams* (pp. 15-29). CRC press.

[119] Eaves, D. (Ed.). (2004). *Handbook of polymer foams*. iSmithers Rapra Publishing.

[120] Jacobs, L. J., Kemmere, M. F., & Keurentjes, J. T. (2008). Sustainable polymer foaming using high pressure carbon dioxide: a review on fundamentals, processes and applications. *Green Chemistry*, 10(7), 731-738.

[121] Wasewar, K. L. (2010). Adsorption of metals onto tea factory waste: a review. *Int J Recent Res* Appl Stud, 3, 303-322.

[122] Berbel, J.; Posadillo, A. Review and analysis of alternatives for the valorisation of agro-industrial olive oil by-products sustainability 2018, 10, 23

[123] Fan, L., Luo, C., Sun, M., Li, X., & Qiu, H. (2013). Highly selective adsorption of lead ions by water-dispersible magnetic chitosan/graphene oxide composites. Colloids and Surfaces B: *Biointerfaces*, 103, 523-529.

[124] Vaillard, A.-S., et al., Confinement and Cross-Linking of 1, 2-Polybutadiene in Two Dimensions at the Air–Water *Interface.* 2020. 36(4): p. 862-871.

[125] Danish, M., Hashim, R., Ibrahim, M. M., Rafatullah, M., & Sulaiman, O. (2012). Surface characterization and comparative adsorption properties of Cr (VI) on pyrolysed adsorbents of Acacia mangium wood and Phoenix dactylifera L. stone carbon. *Journal of Analytical and Applied Pyrolysis*, 97, 19-28.

Appendices

Appendix A

Tables

Table 3.1

provides an overview of the optimum adsorption characteristics for Pb(II) ions

Adsorbent	Adsorption %	Parameters
		pH, time (min), concentration (ppm), dose (mg) , Temp (°C)
LHMDIC	99.95%	5.5, 5, 50, 50,10
LPDIC	98.75%	8, 5, 30, 40, 10

Table 3.2

Values for LHMDIC polymer in the Langmuir model

Concentration (ppm) C_i	$[Pb^{2+}]$ (ppm) C_f	q_e	$1/C_e$	1/q
5	0.935	8.129	1.069	0.123
10	0.639	18.722	1.565	0.053
20	0.409	39.181	2.441	0.026
30	0.433	59.133	2.308	0.017
50	0.462	99.075	2.164	0.010

Table 3.3

Values for LPDIC in the Langmuir model

Concentration (ppm) C_i	$[Pb^{2+}]$ (ppm) C_f	q_e	$1/C_e$	1/q
5	1.178	7.645	0.849	0.131
10	1.400	17.199	0.714	0.058
20	1.419	37.161	0.704	0.027
30	1.515	56.970	0.660	0.018
50	1.202	97.596	0.832	0.010

Table 3.4

Langmuir Adsorption isotherms parameters for Pb(II) on both LHMDIC and LPDIC

Polymer	R^2	Q_{max}	K_1	R_L
LHMDIC	0.8477	5.56	0.067	0.43
LPDIC	0.945	2.43	0.64	0.07

Table 3.5

Values for the LHMDIC polymer in the Friendlish model

Conc (ppm)C_i	Conc (ppm)C_f	q_e	Ln C_e	Ln q_e
5	0.8043	8.129	-0.067	2.095
10	0.747	18.722	-0.448	2.929
20	0.833	39.181	-0.893	3.668
40	0.847	59.133	-0.834	4.079
50	0.662	99.076	-0.778	4.596

Table 3.6

Values for the LPDIC in the Friendlish model

Conc (ppm)C_i	Conc (ppm)C_f	q_e	Ln C_e	Ln q_e
5	1.178	7.645	0.163	0.163
10	1.400	17.199	0.337	0.337
20	1.419	37.161	0.350	0.350
40	1.515	56.97	0.415	0.415
50	1.201	97.597	0.184	0.184

Table 3.7

Friendlish Adsorption isotherms parameters for Pb (II) on both LHMDIC and LPDIC

Polymer	R^2	n	K_f
HMDIC	0.815	0.46	1.28
LPDIC	0.9682	0.49	0.14

Table 3.8

Values for the LHMDIC polymer in the pseudo-first-order model

Time (min)	C_f	q_t	$Ln(q_e - q_t)$
5	0.629	9.686	4.493
10	0.975	9.512	4.495
20	0.899	9.550	4.495
40	0.822	9.589	4.494
60	1.035	9.483	4.495

Table 3.9

Values for the LPDIC in the pseudo-first-order model

Time (min)	C_f	q_t	$Ln(q_e-q_t)$
5	2.577	8.711	4.487
10	2.818	8.591	4.489
20	3.174	8.413	4.491
40	3.129	8.436	4.490
60	3.193	8.404	4.498

Table 3.10

Values for the LHMDIC and LPDIC polymers in the pseudo-first-order model

Polymer	R^2	Theo. q_e	Exp. q_e	K_1
LHMDI	0.319	99.076	0.37	2
LPDIC	0.605	97.597	0.29	5

Table 3.11

Values for the LHMDIC polymer in the pseudo-second-order model

Time (min)	C_f	q_t	t/q_t
5	0.629	9.686	0.516
10	0.975	9.512	1.051
20	0.899	9.550	2.094
40	0.822	9.589	4.173
60	1.035	9.483	6.327

Table 3.12

Values for the LPDIC in the pseudo-second-order model

Time (min)	C_f	q_t	t/q_t
5	2.577	8.711	0.574
10	2.818	8.591	1.164
20	3.174	8.413	2.377
40	3.129	8.436	4.742
60	3.193	8.404	7.139

Table 3.13

Values for the LHMDIC and LPDIC polymers in the pseudo-second-order model

Polymer	R^2	Theo. qe	Exp. qe	K_1
LHMDIC	0.9999	99.076	0.62	0.1
LPDIC	1	97.597	0.61	0.11

Table 3.14

Values for the LHMDIC polymer for the Van't Hoff plot

	Temperature			
Polymer	(°C)	C_f (ppm)	1/T	ln k_d
	5	1.029	0.004	4.567
	10	1.011	0.004	4.585
	20	1.204	0.003	4.410
	40	1.245	0.003	4.377
LHMDIC	60	1.379	0.003	4.275

Table 3.15

Values for the LPDIC polymer for the Van't Hoff plot

	Temperature			
Polymer	(°C)	1/T	ln k_d	
	5	2.284	0.004	3.755
	10	2.032	0.004	3.872
	20	2.687	0.003	3.592
	40	3.117	0.003	3.444
LPDIC	60	3.169	0.003	3.427

Table 3.16

The thermodynamic parameters for the adsorption of Pb(II) on LHMDIC

Temp. (K)	ΔG° (KJ/mol)	ΔH° (KJ/mol)	ΔS° (KJ/mol.K)
278	1.35	- 4.21	- 0.02
283	1.45		
293	1.65		
313	2.05		
333	2.45		

Table 3.17

The thermodynamic parameters for the adsorption of Pb(II) on LPDIC

Temp.	ΔG° (KJ/mol)	ΔH° (KJ/mol)	ΔS° (KJ/mol.K)
278	- 3.1	- 5.88	- 0.01
283	-3.05		
293	-2.95		
313	-2.72		
333	-2.55		

Table 3.18

Concentration of heavy metals using LHMDIC polymer by ICP

Metal ion	Initial Conc. of metal ions (ppm)	Final Conc. of metal ions (ppm) using 50 mg of LHMDIC	Removal %)
Al	275.14	49.025	82%
As	3.306	2.972	10%
B or Ba	126.181	111.273	12%
Bi	0.366	0.219	40%
Cd	0.172	0.007	96%
Cr	330.924	106.927	67%
Co	1.015	0.513	49%
Cu	24.987	2.665	89%

Fe	543.011	119.88	78%
Ni	6.376	3.756	41%
Pb	3.218	0.0262	91%
U	0.258	0.094	64%
Zn	75.845	8.453	89%

Table 3.19

Results of analyzes for the Concentration of heavy metals using LPDIC polymer by ICP

Metal ion	Initial conc.of Jericho sample (ppm)	Final conc. (ppm) using 50 mg Of LPDIC	Removal %
Al	275.14	54.912	80%
Ba	36.714	22.87	38%
Bi	0.366	0.179	51%
Ca	62223.45	44377.007	29%
Cd	0.172	0.014	92%
Cr	330.924	128.61	61%
Co	1.015	0.593	42%
Cu	24.987	3.004	88%
Fe	543.011	133.485	75%
Mn	53.484	39.552	26%
Mo	0.995	0.490	50%
Ni	6.376	3.981	38%
Pb	3.218	0.346	89%
TI	0.008	0.002	75%
U	0.258	0.114	56%
Zn	75.845	13.94	82%

Appendix B

Figures

Figure 3. 1
Some of the polyphenolic compounds present in OILW

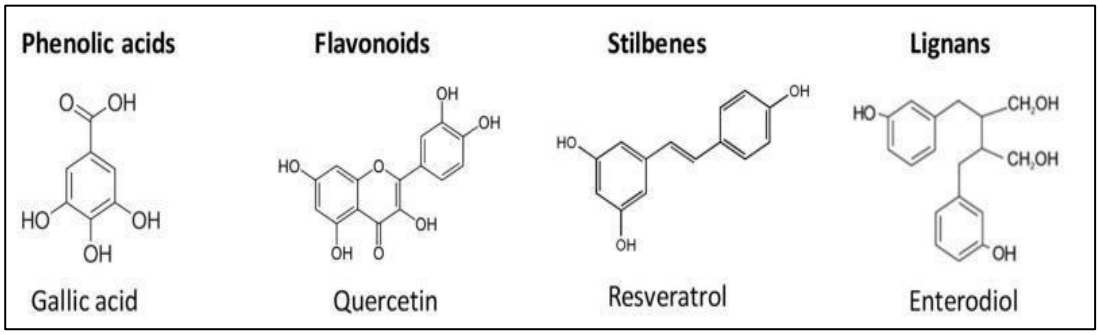

Source: Fan, L., Luo, C., Sun, M., Li, X., & Qiu, H. (2013).

Figure 3.2

A representative structure of foam made form isocyanates and OILW components

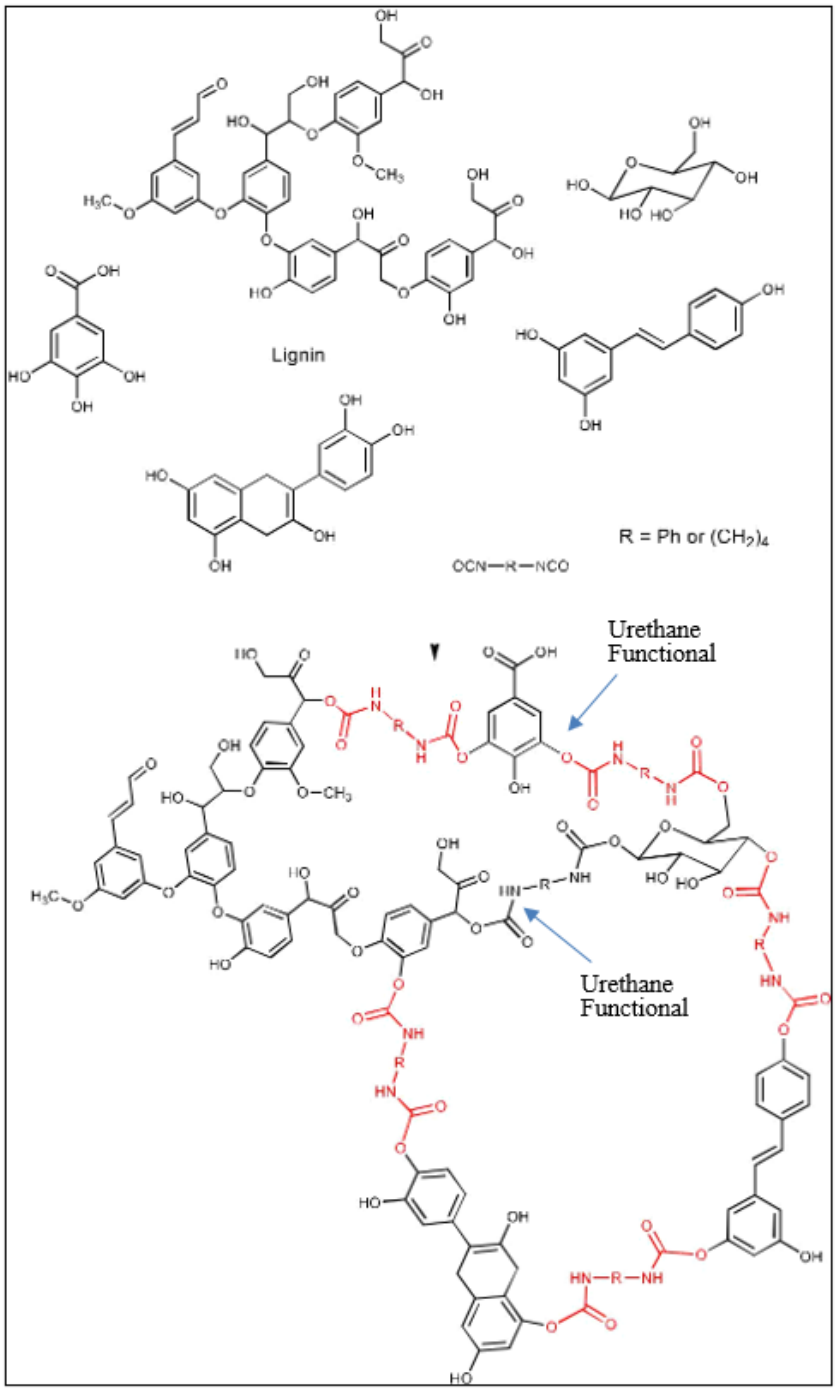

Figure 3.3

Thermal gravimetric analysis for LHMDIC

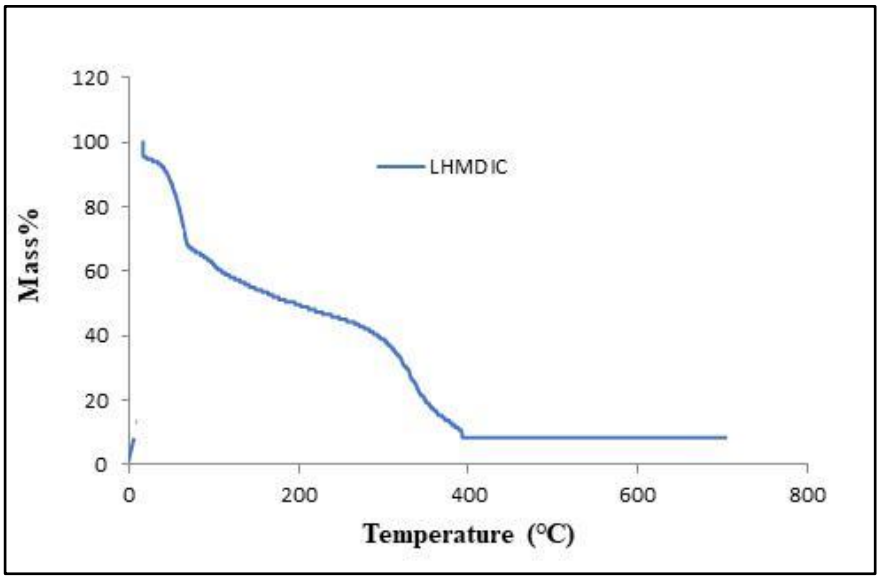

Figure 3.4

Thermal gravimetric analysis for LPDIC

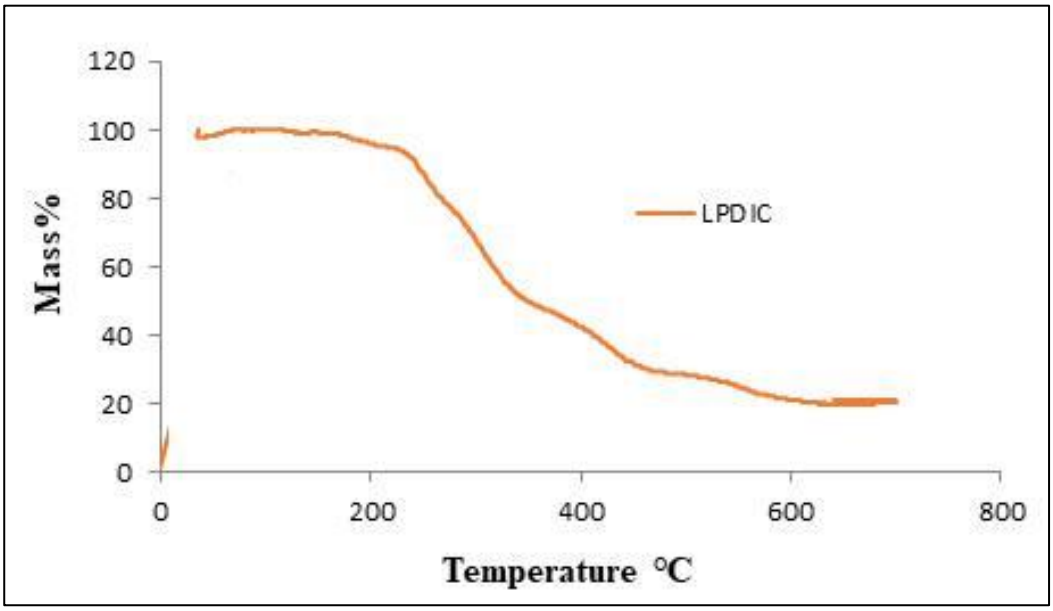

Figure 3.5

FT-IR of LHMDIC

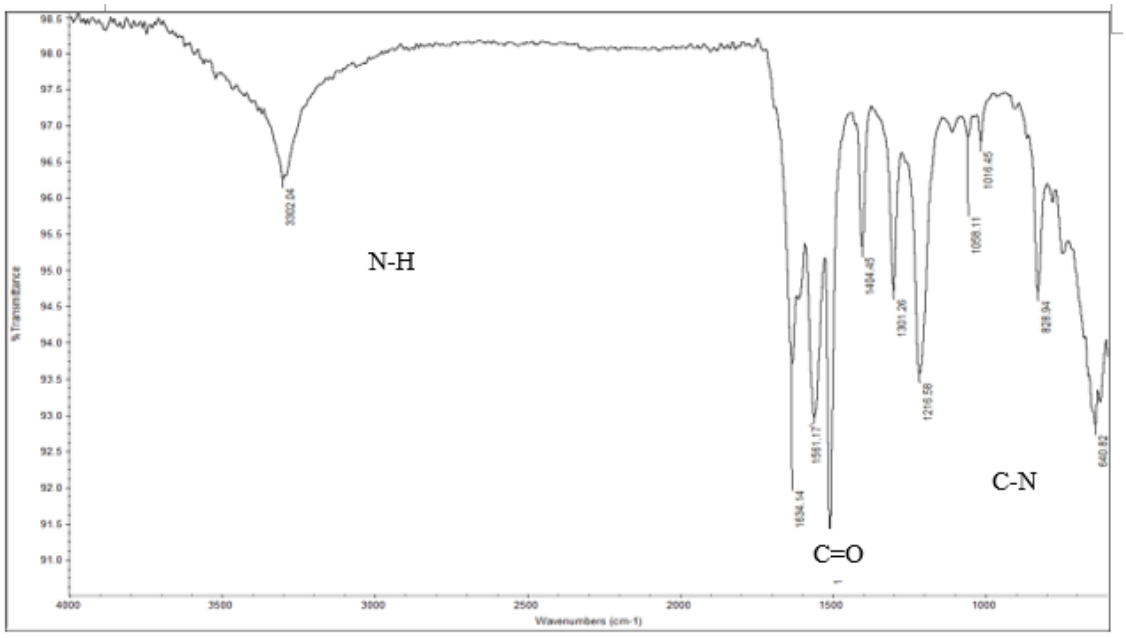

Figure 3.6

FT-IR of LPDIC

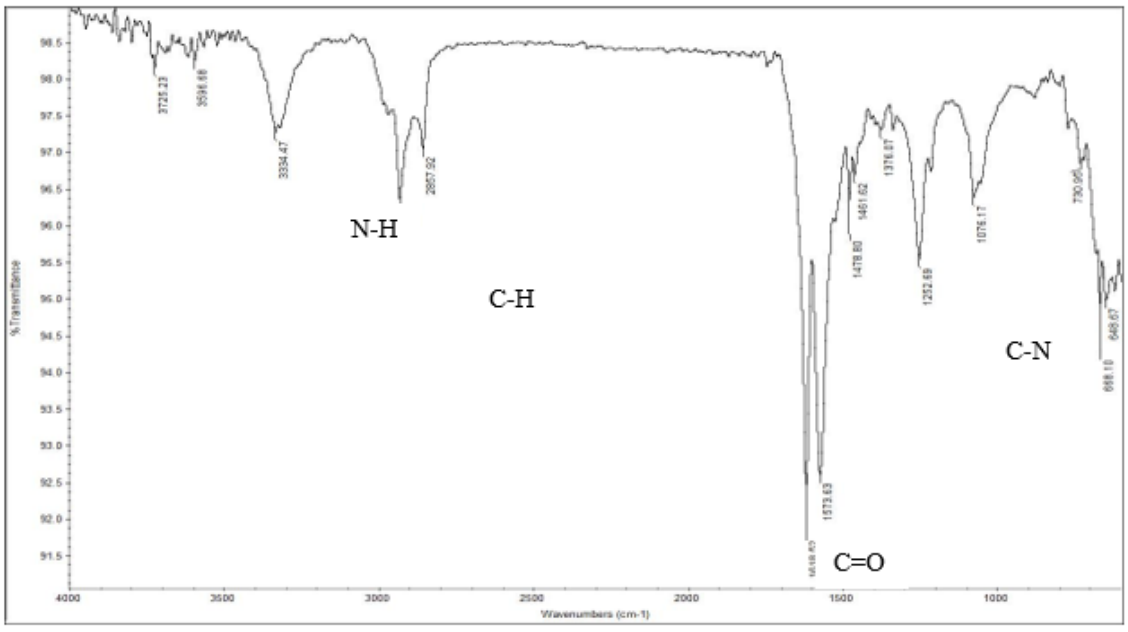

Figure 3.7
FT-IR of LPDIC with wastewater after adsorption

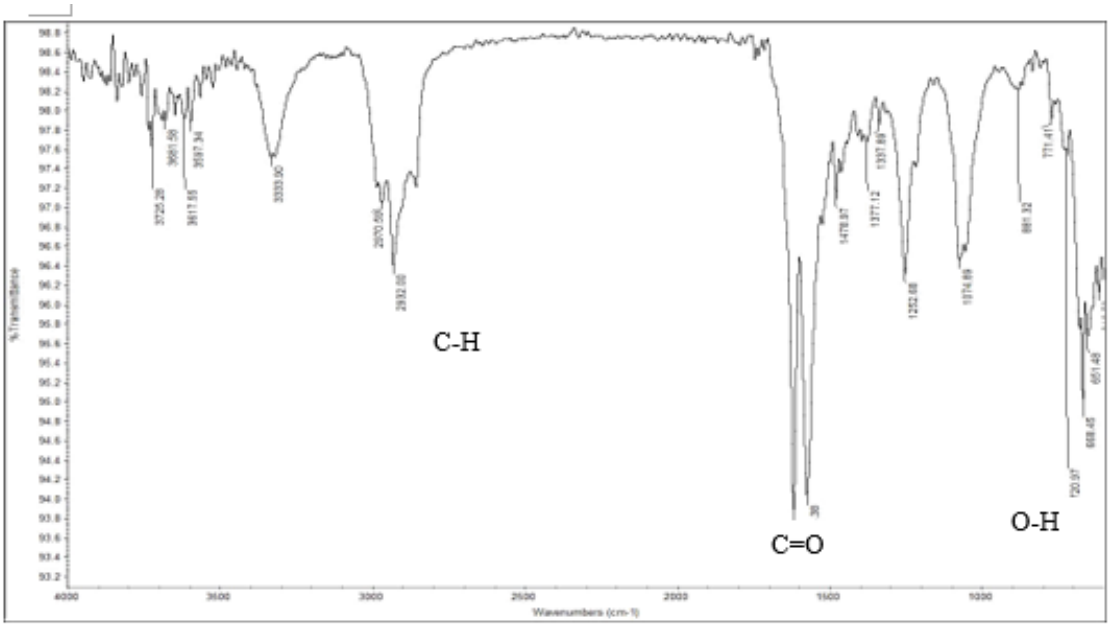

Figure 3.8
FT-IR of_LHMDIC with wastewater after adsorption

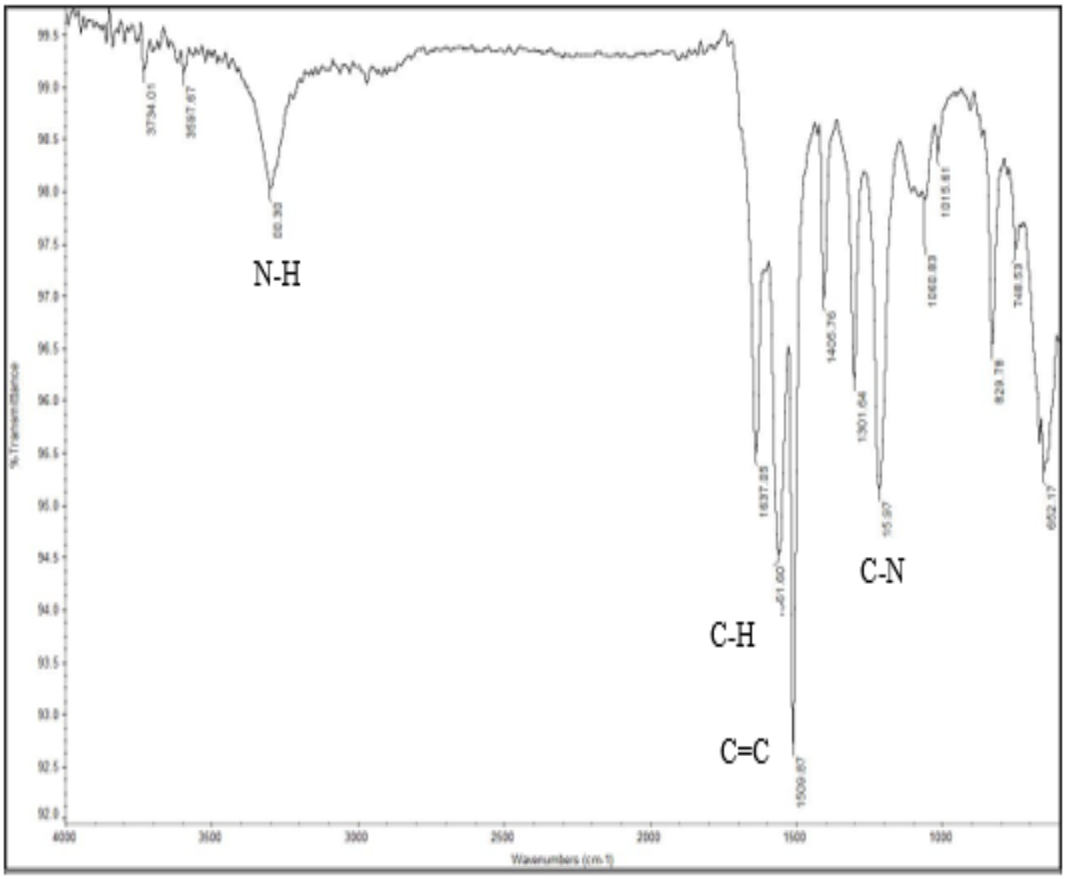

Figure 3.9

Atomic force microscope image for deritivized OILW

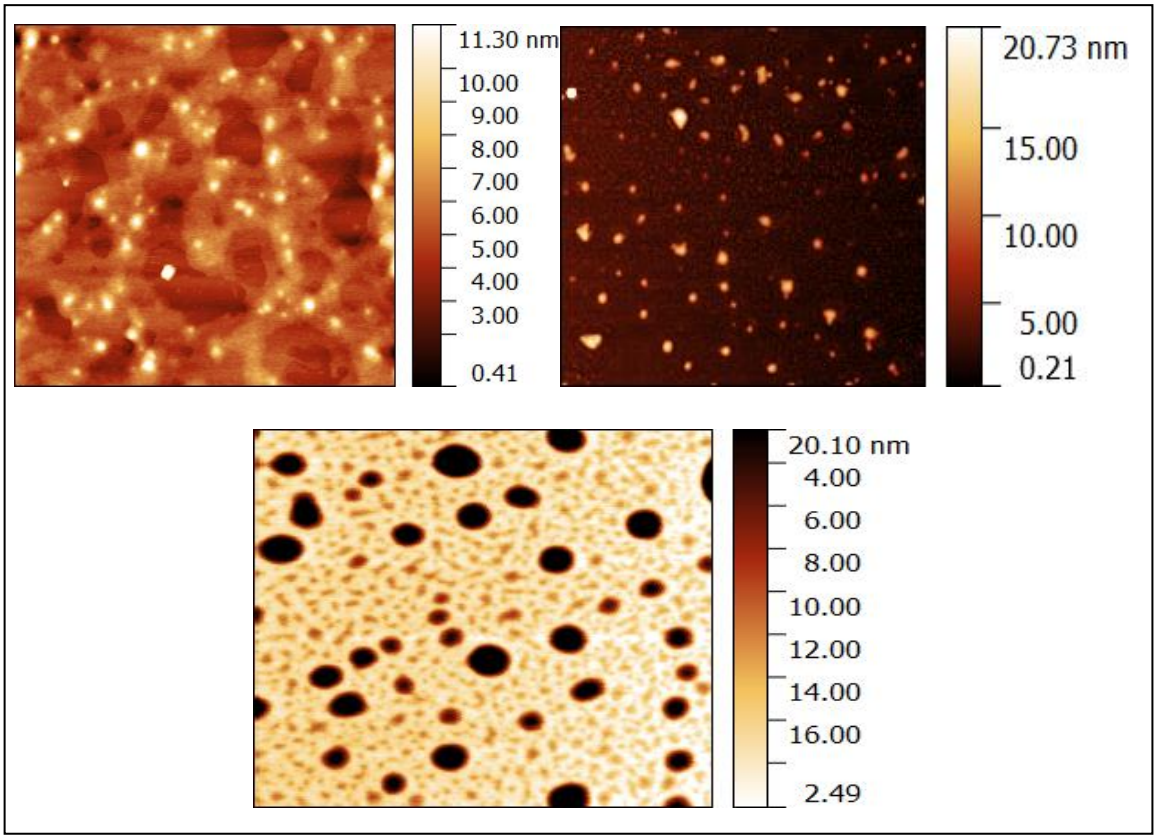

Note: A) Atomic force microscope image for OILW/ 1,4-hexamethylene diisocyanate (LHMDIC) B) Atomic force microscope image for OILW/1,4-phenylne diisocyanate (LPDIC)

Figure 3.10

Effect of pH on the adsorption of Pb(II) on both LHMDIC and LPDIC

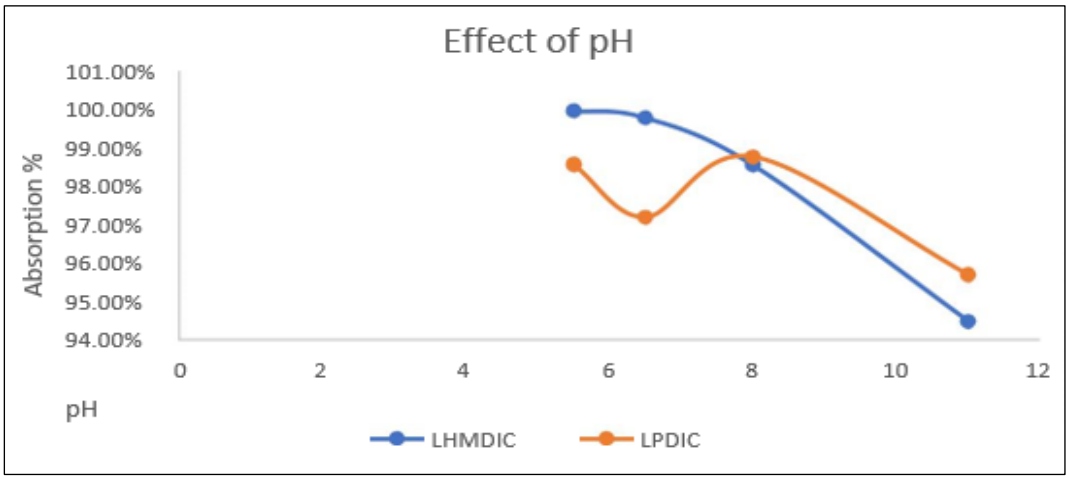

Figure 3.11

Effect of dose on the adsorption of Pb (II) on both LHMDIC and LPDIC

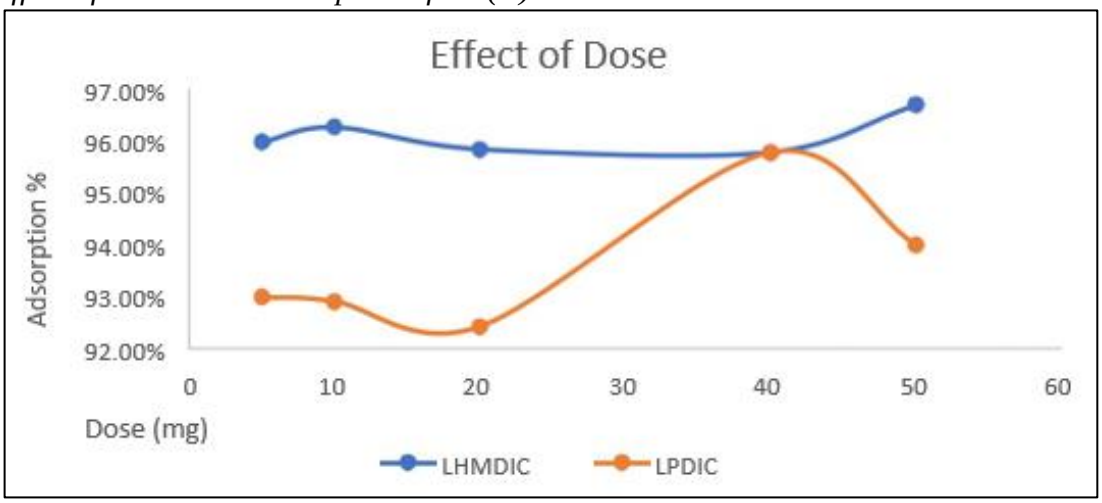

Figure 3.12

Effect of concentration on the adsorption of Pb (II) on both LHMDIC and LPDIC

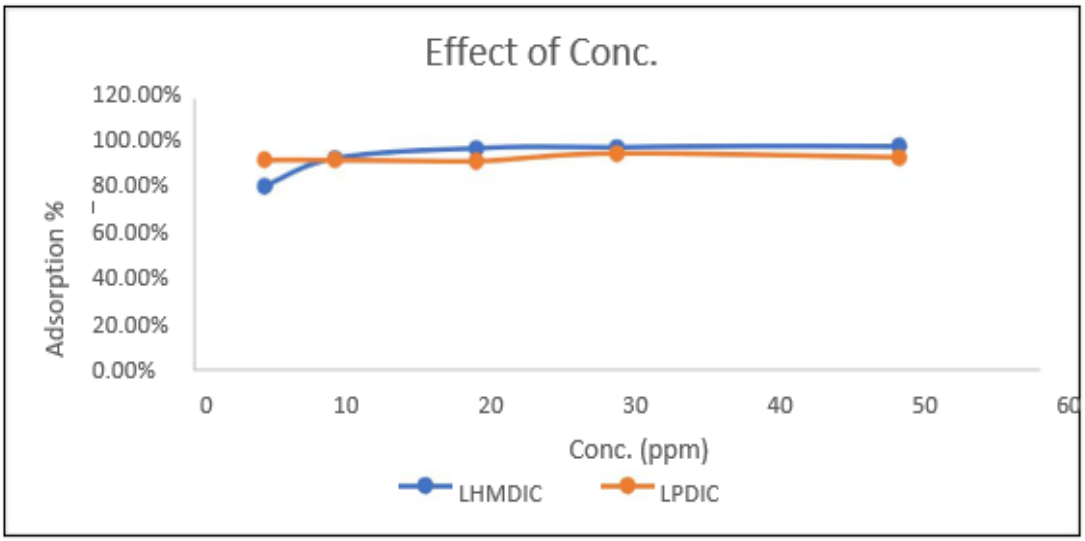

Figure 3.13

Effect of time on the adsorption of Pb (II) on both LHMDIC and LPDIC

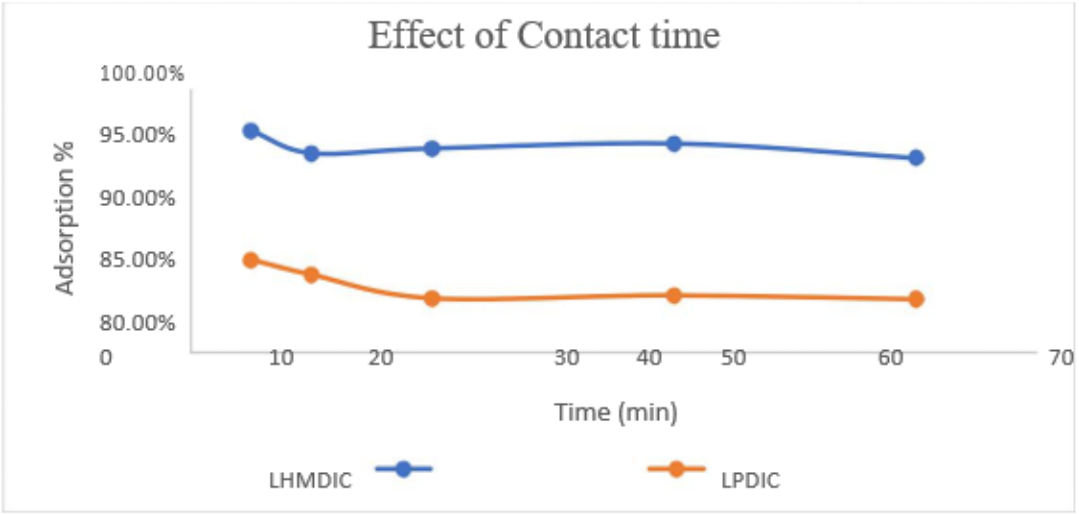

Figure 3.14

Effect of temperature on the adsorption of Pb(II) on both LHMDIC and LPDI

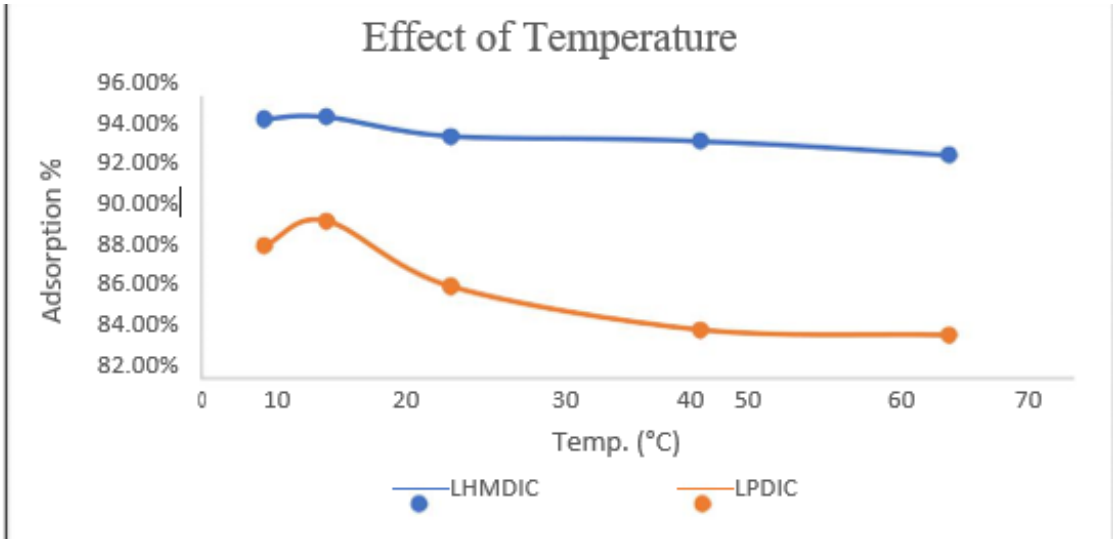

Figure 3.15
Langmuir model for adsorption of Pb(II) on both LHMDIC and LPDIC

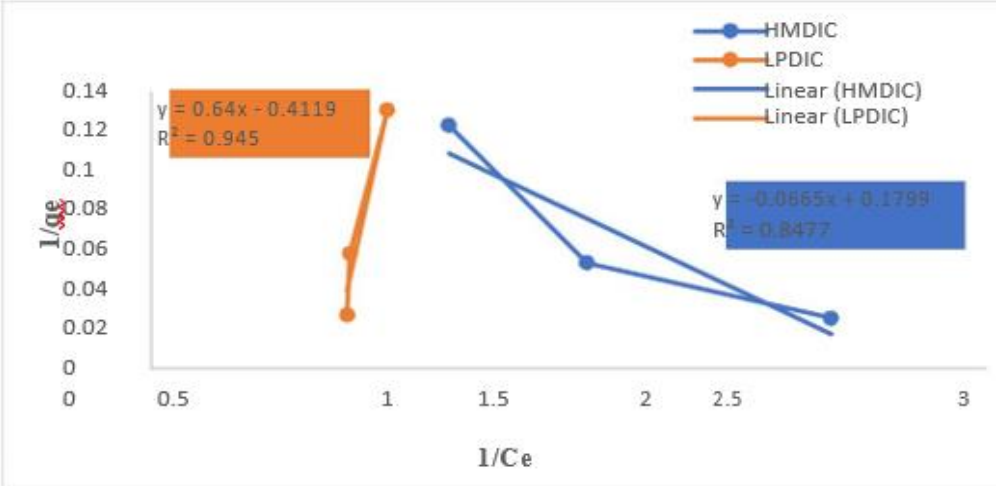

Figure 3.16
Friendlish model for adsorption of Pb(II) on both LHMDIC and LPDIC

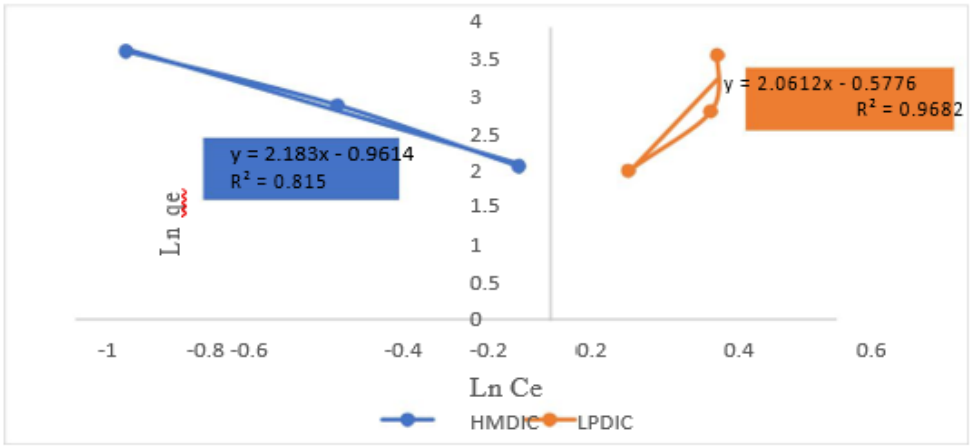

Figure 3.17
pseudo-first-order model for adsorption of Pb(II) on both LHMDIC and LPDIC

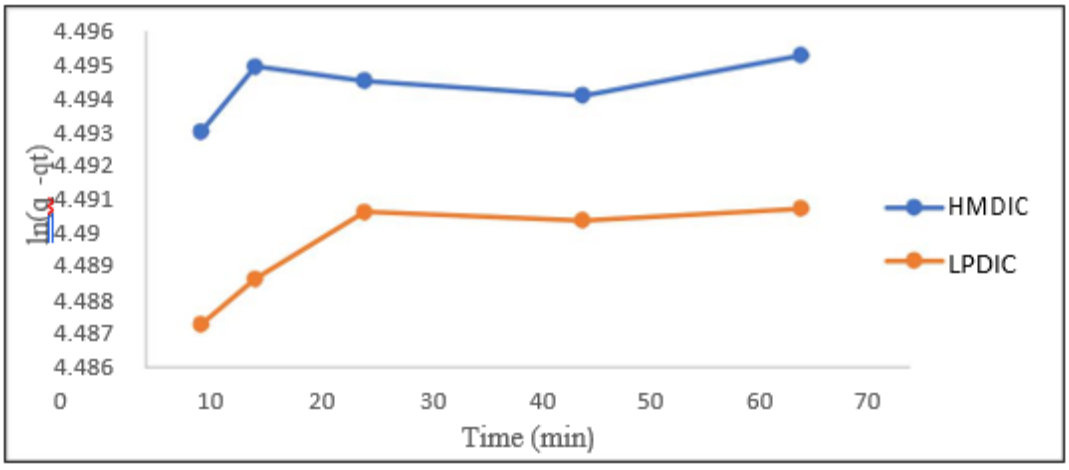

Figure 3.18

pseudo-second-order model for adsorption of Pb (II) on both LHMDIC and LPDIC

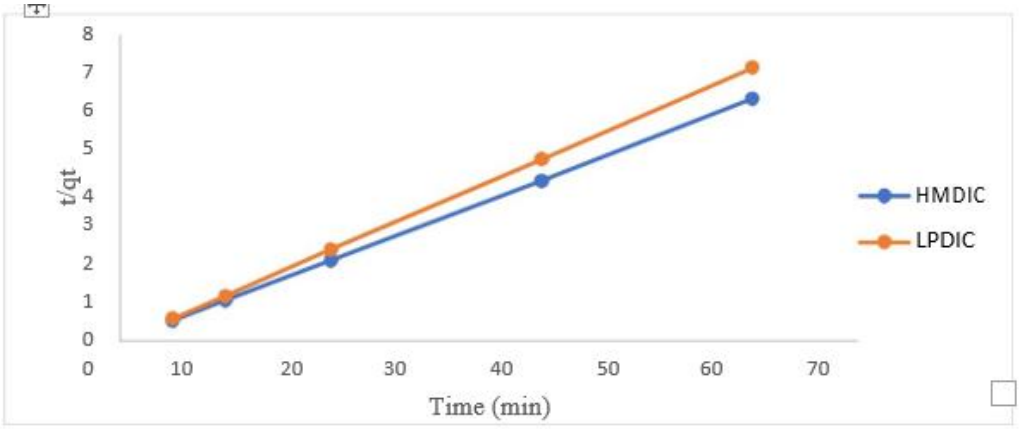

Figure 3.19

Van't Hoff plot for adsorption of Pb(II) on both LHMDIC and LPDIC

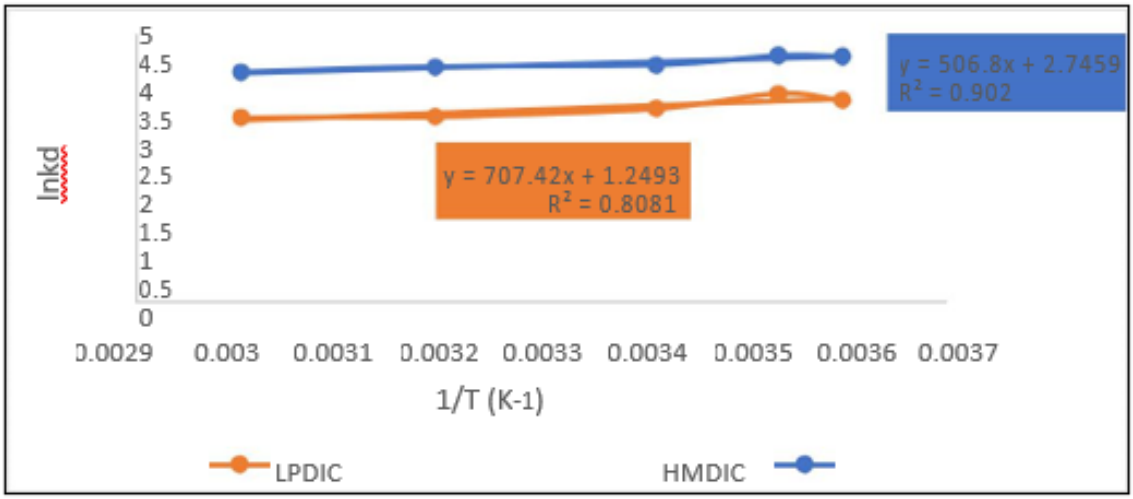

جـامعـــة النجاح الوطنية

كليـــة الدراســـات العليـــا

التحلل التحفيزي للمخلفات السائلة لصناعة الزيتون من أجل إنتاج مضادات أكسدة فينولية

إعداد

إسراء اشريدة

إشراف

أ.د. عثمان حامد

د .عبد الفتاح الملاح

قدمت هذه الرسالة استكمالا لمتطلبات الحصول على درجة الماجستير في العلوم البيئية، من كلية الدراسات العليا، في جامعة النجاح الوطنية، نابلس- فلسطين.

2023

التحلل التحفيزي للمخلفات السائلة لصناعة الزيتون من أجل إنتاج مضادات أكسدة فينولية

اعداد

إسراء اشريدة

إشراف

أ.د.عثمان حامد

د.عبد الفتاح الملاح

الملخص

يعد تلوث المياه من أهم التحديات في العالم، خاصة التلوث بالمعادن الثقيلة .أثبتت الفاعلية العالية لأيونات المعادن الثقيلة، حتى عند التراكيز القليلة، أنها تتطلب إجراءات االمتزاز بشكل خاص، والتي تعتبر أيضاً أقل تكلفة من األلساليب التقليدية .تمتاز الممتزات التي خضعت لتعديل كيميائي بان لها مساحة سطح كبيرة وقدرة امتصاص من مياه الصرف الصحي باستخدام اللجنين أعلى من الممتزات غير المعدلة .تم اختبار إزالة أيونات الرصاص ، والنفايات الطبيعية ، وبعض أشكاله المعدلة.

الهدف الرئيسي من هذه الدراسة هو الإستفادة من خصائص رغوة البولي يوريثان، المحضر مخبرياً، والذي يمتاز بأنه من المواد سهلة التحضير وذات الكفاءه العالية الستخدامه كمادة ماصة لمعدن الرصاص السام في معالجة المياه الملوثة من مخلفات الزيتون الصناعية السائلة.

في هذه الدراسة تم استخالص اللجنين الموجود في البقايا السائلة لعصارة الزيتون وتحويله إلى مركبين رغويين من البولي يوريثان المعدل بمجموعة وظيفية أيونية مرتبطة به تساهمياً. يتم تحضير المركب الأول عن طريق بلمرة مركب 1-6 هيكساميثيلين ثنائي أيزوسيانات مع الليغنين المستخلص المؤكسد بإضافة DMF وكمية من ثالث ايثانول الأمين. وبنفس الطريقة تم بلمرة 1-4 ثنائي أيزوسيانات الفينلين النتاج الرغوة المحضرة وهي مادة جديدة ذات كفاءه فريدة ومميزة لتنقية مياه الصرف الصحي.

تم تشخيص البوليمرات المحضرة باستخدام TGA وFT–IR ثم استخدامها في استخالص الأيونات المعدنية من مياه الصرف الصحي. تم تحديد ظروف االمتزاز المختلفة التي تعطينا أعلى فعالية من خالل تجارب مخبرية مثل: الرقم الهيدروجيني، ووقت التالمس ودرجة الحرارة، وكمية المادة، والتركيز الأولي أليون المعدن.

تم تقييم تأثير العوامل المختلفة مثل تركيز أيون الرصاص ودرجة الحرارة ودرجة الحموضة وكمية الماده ووقت التالمس لتحديد ظروف االمتزاز المثلى .كانت القيمة المثلى للمعلمات التي تم فحصها لـ LHMDIC حوالي 5.5 درجة حموضة، جرعة 50.00 مجم، تركيز 50.00 جزء في المليون، 5.00 دقيقة من وقت التالمس، و10 درجات مئوية. كانت الظروف المثالية لـ LPDIC هي أألس الهيدروجيني 8، جرعة 50.0 مجم، تركيز50.00 جزء في المليون ، 5.00 دقيقة من مدة التالمس، و10 درجة مئوية.

تم تحديد كفاءة الإزالة القصوى لتكون99.95 ٪ لـ HMDIC و98.75 ٪ لـ LPDIC. أظهر هذا التطبيق لكفاءة إزالة أيونات Pb (II) لعينة من مياه الصرف الصحي عملية إزالة متميزة .يبدو أن أيون Pb (II) يتبع ترتيب الثانية الزائفة في امتزاز أيون Pb (II) على بوليمرات LHMDIC وLPDIC ألن = (R^2 (0.9999) و (1 = R^2) ، على التوالي .تتبع كال الفومتين نموذج النجمويرر، حيث أن كال القيمتين R2 الظاهرة قريبة جدا من 1. قيم ° G لكال الرغوة سلبية، مما يشير إلى أن امتصاص أيونات Pb (II) على بوليمرات LPDIC يكون تلقائياُ.

اثبتت هذه الدراسة ان البوليمرات المحضرة مخبريا لها كفاءة عالية في ازالة ايونات الرصاص السامة من مخلفات النفايات السائلة كما انها تمتاز بتكلفتها القليلة وببساطتها.

الكلمات المفتاحية: االمتزاز، الزيت، الرصاص، اللجنين، رغوة اليوريثان، النفايات السائلة لصناعة الزيتون.